

Final Report – Marshall Plan Scholarship

Development of a Human *in vitro* Model for *Pseudomonas aeruginosa* Infection in Cystic Fibrosis

Supervisor at TU Wien

Prof. Peter Ertl, Univ.Prof. Dipl.-Ing. Dr., Head of the cooperative cell chip group between the Institute of Applied Synthetic Chemistry and the Institute of Chemical Technologies and Analytics

Supervisor at Host Institution

Prof. Laurence Rahme, Ph.D., Assoc. Professor of Surgery, Microbiology and Immunobiology at Harvard Medical School and Director of the Molecular Surgical Laboratory, Department of Surgery, Massachusetts General Hospital

by

Doris Roth, BSc

Matriculation No. 01121186

Cambridge MA, Tuesday 21st of May 2019

Abstract

Engineered human microtissues provide a window into structure-function relationships that underlie organ function, drug responses, and pathologies. The aim is to recapitulate both native tissue architecture and the organotypic mechano-chemical microenvironment to enable the study of dynamic interactions and emergent functions as well as disease states, for example in Cystic Fibrosis (CF). Specifically, engineered CF lung microtissues can help identify mechanisms and develop diagnostics for the onset and progression of *Pseudomonas aeruginosa* infection in CF disease. Here, we discuss the development of a patient cell-based *in vitro* model of CF airway inflammation, the CF Airway Chip, that emulates and enables the patient-specific, real-time study of the interactions between mucociliary function, immune cell responses, and bacterial infection onset and progression. In the future, such a model can help us understand the role of patient-specific inflammatory responses and immune cell recruitment in shaping cystic fibrosis disease states

Table of Contents

Abstract	i
Table of Contents.....	ii
1 Introduction	1
1.1 The Immune System, <i>Pseudomonas aeruginosa</i> and the Cystic Fibrosis Airway	2
1.2 Current Airway models.....	3
1.3 Organs-on-a-Chip	5
1.4 Approach	6
2 Materials and Methods.....	7
2.1 Organ Chips.....	7
2.2 Instrumental Setup.....	8
2.3 Chip Fabrication.....	10
2.4 Healthy primary airway epithelial cell culture.....	11
2.4.1. Cell Expansion.....	11
2.4.2. Transwell Controls	14
2.4.3. S-1™ Chip cultures.....	14
2.5 Cystic Fibrosis airway epithelial cell culture	18
2.5.1. Cell Expansion.....	18
2.5.2. ECM coating	18
2.5.3. Transwell culture.....	19
2.5.4. Chip cultures.....	19
2.5.5. Open Top Chip Culture	20
2.5.6. S1-Chip culture	20
2.6 Immunofluorescence Staining.....	21
2.7 Lactate Dehydrogenase Cytotoxicity Assay	22
2.8 High-Speed Video Microscopy.....	22
2.9 Ciliary Imaging	22
2.10 Bead Transport.....	23
2.11 Image Analysis	23
3 Results.....	23
3.1 Emulating the Healthy Human Airway	23
3.2 Emulating the Cystic Fibrosis Airway	31
4 Discussion	38

5	References	39
6	Attachments.....	a

1 Introduction

In cystic fibrosis (CF) patients, genetic mutations in the cystic fibrosis transmembrane conductance regulator (CFTR) gene (Cytogenetic Location: 7q31.2) cause multiple organ manifestations such as pancreatic insufficiency, diabetes and obstructive lung disease from infancy with chronic bacterial infections, the lung disease being the main cause of morbidity and mortality¹. The key disease manifestations in the human lung are delayed mucociliary clearance through airway surface liquid depletion, abnormalities of the physical properties and adhesion of mucus, predisposition to chronic microbial infection due to abnormal mucosal defenses, and dysregulated inflammation that almost always leads to irreversible lung injury¹. While it is well-known that a combination of these factors underlies initiation and perpetuation of chronic infection and inflammation, the precise role and timing of individual factors remains unclear. In particular, due to the lack of suitable animal and *in vitro* models of CF airways, we do not fully understand whether destructive airway inflammation is a consequence or can also be the cause of increased susceptibility to chronic infection¹. A recent study suggests that early CF lung disease is characterized by an increased mucus burden and inflammatory markers without infection or structural lung disease².

In the human bronchial and small airway epithelium, ciliated cells are highly polarized and beat their cilia in a coordinated fashion through a lubricating substance, the periciliary liquid (PCL). This PCL-lubricated ciliary beat enables the unidirectional and efficient transport of the overlying mucus secreted by interspersed goblet cells. The so-called mucociliary escalator traps and clears pathogens and toxins out of the lungs and is essential for physiological lung function. The perturbation of CFTR-mediated fluid secretion and ion gating alters the salt composition of the mucus and, in consequence, increases mucus viscosity^{3,4}. Due to the increased “stickiness” of the mucus, mucociliary transport is greatly impaired, which is hypothesized to generate mucus buildup that not only impedes breathing but also renders the patient susceptible to chronic lung infection with pathogens, particularly the bacterium *Pseudomonas aeruginosa*⁵⁻⁷. Furthermore, CFTR defects are known to increase fluid and sodium absorption via the epithelial Sodium Channel (ENaC), which is thought to exacerbate the depletion of the lubricating periciliary layer and further impair mucociliary transport⁸. According to one hypothesis, the great sensitivity of the periciliary layer to the altered osmolar forces of the overlying mucus eventually causes the periciliary layer to collapse, ensuing in failure of mucociliary transport⁹. The stagnant mucus environment could thus enable pathogens, such as *P. aeruginosa*, to take hold and form

permanent biofilms^{7,10}. In addition, decreased bicarbonate transport through CFTR is thought to condense the mucus and decrease the pH in the human airway, which may affect host immune cell activities and contribute to deficiencies in pathogen defense^{11–13}. It is possible that CF epithelium elicits resident immune cell activation even without the presence of infections, causing harmful immune responses^{1,2,14,15}. Conversely, the presence of bacterial biofilms in turn could elicit harmful immune responses and cause tissue remodeling that further impairs mucociliary transport¹⁶.

In sum, mucociliary transport, *P. aeruginosa*, and host immune cells engage in very complex interactions in CF airways, and their sequence and causalities remain unclear. Further, while Cystic Fibrosis is caused by the defect of a single gene, according to the CFTR2 database (<https://cftr2.org/>), 346 different CF causing mutations have been identified, each of which might change the relative role of the factors involved in lung pathogenesis. Since the discovery of the gene defect in 1989, which was published in a series of three publications^{17–19}, more than 2000 genetic variants of CFTR have been discovered. Different mutations and combinations of mutations cause different disease phenotypes in an autosomal recessive monogenetic fashion, with the F508del variant being the most common mutation causing Cystic Fibrosis²⁰. A high variability in phenotype and a broad range of disease severity are observed even in patients carrying the same genotype²¹.

This research project aims to address these challenges by developing a patient-cell based dynamic 3D *in vitro* model of the CF airway, the CF Airway Chip, that recapitulates and enables the patient-specific, real-time study of the interactions between mucociliary function, immune cell responses, and bacterial infection onset and progression. Furthermore, biomechanical readouts methods have been developed to describe the CF mucociliary escalator.

1.1 The Immune System, *Pseudomonas aeruginosa* and the Cystic Fibrosis Airway

The airway epithelium, the immune system and the pathogen *Pseudomonas aeruginosa* engage in complex interactions leading to disease exacerbations and mortality in patients with Cystic Fibrosis. The respiratory tract is home to a number of resident and circulating immune cells, including natural killer cells, macrophages, mast cells, dendritic cells, neutrophils and lymphocytes that continuously protect the lung tissue from pathogens and foreign particles entering the lung²². In CF patients, unresolved neutrophilic inflammation and recurrent pulmonary infections lead to lung disease, disease exacerbations and structural lung damage.

Studies show that even in the absence of infection with pathogens, abnormalities of the CF airway mucus, such as increased viscosity, can already lead to a proinflammatory environment, hypoxia and oxidative stress². Excessive neutrophil-dominated inflammation is observed¹ and neutrophil elastase activity was associated with early bronchiectasis in children²³. Findings of elevated neutrophil elastase levels and other inflammatory markers such as IL- β , IL-8 and TNF- α in the airway and studies on CF fetuses suggest that inflammation precedes infection whereas other studies argue that inflammation is secondary to infection²⁴.

Chronic neutrophil-mediated inflammation following infection can markedly reduce airway surface liquid (ASL) height^{1,25} affecting the mucociliary escalator. Further, the accumulation of large amounts of DNA derived from neutrophils and actin increases mucus viscosity and negatively impacts mucociliary clearance²⁴. A key component of this dysregulation is NETosis, a special form of cell death, that leads to the release of neutrophil extracellular traps (NETs). NETs are networks of primarily DNA and actin associated with granules, such as the protease neutrophil elastase, that trap pathogens²⁶. In CF, neutrophils and *P. aeruginosa* induced NETs are incapable of clearing the infection and in fact even favor bacterial colonization and the formation of biofilms, and clinical strains can acquire resistance to NET-mediated killing²⁴. *P. aeruginosa* can undergo microevolution and adapt to develop multi drug resistances as shown in the analysis of isolated strains from a CF patient over the course of 8 years²⁷. The microaerophilic environment of the CF lung presents a hostile environment to *P. aeruginosa* resulting in the formation of low oxygen tension biofilms^{28,29}. *P. aeruginosa* biofilms are associated with excessive inflammation, recurrent exacerbations and accelerated decline in lung function and ultimately increasing mortality. To date, no effective treatment options of recurrent PA infection in CF exist. Hence, platforms that enable the study of host-pathogen interaction upon *P. aeruginosa* infection of the CF airway, biofilm formation, dysregulated immune reaction, elevated neutrophil infiltration and NETosis on human physiology are desperately needed.

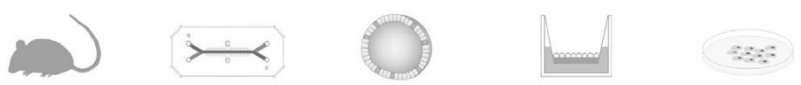
1.2 Current Airway models

Cystic Fibrosis research is carried out on a variety of animal and *in vitro* models that are essential for drug discovery, drug testing and foundational research. Each model has specific advantages and challenges when mimicking the human physiology of the CF lung (fig 1). Soon after the discovery of CFTR, CF mouse models were developed and mice are now widely used model organism for CF research, especially for the intestine. However, mice models homozygous for the most common F508del mutation were thought to not show any abnormalities in lung function³⁰.

Recent studies suggest that CF mouse models do show very specific abnormalities in lung function but fail to mimic the severity and scope of the human disease condition³¹. Furthermore, the tissue composition and function differ vastly between mice and humans, including differences in epithelial cell composition, cartilage architecture, smooth muscle biology, and altered electrophysiology³¹. For example, the proportions of mucus producing goblet cells, secretory club cells, and ciliated cells differ between mice and humans³¹. Lastly, mouse models infected with human pathogens do not recapitulate the disease states and infection response of a CF patient, hence insufficiently representing the complex nature of host-pathogen interactions in humans³¹. Other animal models such as the CF pig and CF ferret recapitulate the full spectrum of CF phenotype in human patients and closely resemble to human lung cell biology³². The CF ferret covers a wide range of abnormal airway function for the study of CF but does not exhibit ENaC dysregulation and disease severity is greatly increased compared to humans. Both the CF ferret and the CF pig require high maintenance and intensive medical treatment to increase their lifespan³¹. CF rats are promising model organisms but need further characterization.

To resemble human biology more closely, human *in vitro* airway cell models are increasingly being used in CF research with human cells cultured at air liquid interface on transwell™ supports. This emerged to being the gold standard for airway *in vitro* models as opposed to undifferentiated submerged 2D cultures. Immortalized cell lines like Calu-3 from adenocarcinomas or CRISPR-Cas9 gene edited cell lines are used to study the role of CFTR³². The more preferred and used *in vitro* model for CF research are primary cells, progenitor cells obtained from human tissue, that can be differentiated into pseudostratified airway epithelium³³. Although challenging, there are promising approaches for the use of differentiated induced pluripotent stem cells (iPSCs) for airway *in vitro* models^{32,34}.

Among those exceptional advances in stem cell research are organoids. Organoids are progenitor cells that self-assemble to form differentiated tissue spheroids with an internal lumen³⁵. The organoid technology enables the easy testing of the efficacy of CFTR modulator and corrector drugs using a swelling assay, where the recovery of CFTR function is indicated by an increase of the luminal diameter in intestinal organoids^{36,37}. These new approaches in 3D cell culture models are accompanied in their novelty by the organ-on-a-chip technology and more specifically in the context of the healthy airway the small airway-on-a-chip^{38,39}. Organ-chips are 3D *in vitro* microfluidic cell culture platforms that emulate the mechanochemical microenvironment and the 3D architecture of human tissue. Dynamic chip cultures resemble *in vivo* human physiology more closely compared to static 3D transwell cultures. A more detailed description of the Airway-Chip can be found in section 2.1..



	Animal	Lung-on-Chip	Organoid	Air Exposed Primary Cells	2D Cell Line
3D tissue architecture	●●●	●●○	●●○	●○○	○○○
Full cell differentiation	●●●	●●○	●●○	●●○	●○○
Hemodynamic environment	●●●	●●●	○○○	○○○	○○○
Circulating immune cells	●●●	●●○	○○○	●○○	○○○
Physiological biomechanics	●●●	●●○	●○○	●○○	○○○
Long-term viability	●●●	●○○	●●○	●●○	●●●
Familiarity	●●●	●○○	●●○	●●●	●●●
Access to luminal space	●●○	●●●	●○○	●●●	○○○
Patient-specific cells	●○○	●●●	●●●	●●●	●●●
Conserved disease phenotype	○○○	●●○	●●○	●○○	●○○
Throughput	○○○	●○○	●●○	●●○	●●●

Figure 1 Comparison of experimental strategies for lung modeling taken from Nawroth et al 2018⁴⁰. Whereas animal models enable *in vivo* studies they do not resemble human physiology and in particular diseased phenotypes. High maintenance efforts and the ethical need to minimize the use animals lower the throughput of studies. The Lung-on-Chip uses human cells that can be patient specific and incorporates differentiated epithelium and endothelium as well as circulating immune cells. The microfluidic channels in the chip create tissue-tissue interfaces and mimic the *in vivo* hemodynamic environment. The complexity and novelty of the chip reduces the throughput and familiarity. Organoid cultures self-assemble and allow the study of patient derived airway epithelium. The spheroid shape with an internal lumen excludes infection modeling and the study of mucociliary clearance. Air exposed primary cells in transwell cultures have standardized culture protocols and are easy to use. Transwell cultures are highly characterized and allow the use of patient specific cells. The static culture model does not mimic the mechanical microenvironment crucial for full differentiation especially for endothelial cells. 2D submerged cell lines are of great use for CFTR-related research but highly limited for translational research.

1.3 Organs-on-a-Chip

Organs-on-a-chips (OOCs) are engineered microtissues coupled with microfluidic devices emulating native tissue architecture and the mechanochemical environment of an organ. OOCs emerged from collateral advances in microfabrication in the semiconductor industry, stem cell technology and human tissue engineering. The microenvironment includes multiple cell types enabling tissue-tissue interfaces as well as allowing for controlled involvement of mechanical forces such as stretch and shear, fluid flow, biochemical cues and electrical or optical signals^{40–43}. The design of OOCs is guided by the applications that the organ model should host such as key physiological functions and readouts with spatio-temporal resolution. Hence, they do not attempt to mimic a full organ. The goal is to provide a complex physiological model, yet one simple enough to facilitate reproducibility, manipulation and control.

Inside the chips are cells growing on porous membranes in interfacing microfluidic channels. This enables the establishment of cell-cell and subsequently tissue-tissue interactions that resemble human physiology more closely than conventional 2D culture models. It has been shown that endothelial and mesenchymal cells modulate differentiation of epithelial cells towards the development of an adult airway epithelium⁴⁰, tissue growth and cell activation during inflammation. The ability to perfuse OOCs enables the incorporation of circulating immune cells that can migrate to the epithelium upon the activation of the underlying epithelium⁴² and the dynamic flow of nutrient-containing liquids and gases exerts shear stresses such as those experiences within small vessels⁴⁴ adding further to their physiological relevance. Endothelial cells are constantly exposed to forces, such as gravitational forces, mechanical stretches, stress and shear stress. Physiological shear stress experienced through blood flow and the flow pattern have been shown to modify morphology, gene expression and metabolism of endothelial cells⁴⁵⁻⁴⁷. In addition, the lung epithelium is subject to dynamic stresses, stretches and pressure changes during breathing. It has been shown that low levels shear stresses enhance epithelial barrier function⁴⁸ and mechanical forces experienced by epithelium are key regulators during lung development⁴⁹⁻⁵¹. The small-airway-on-a-chip described by Benam et al.⁵² consist of a differentiated mucociliary airway epithelium and a microvascular endothelium in a manipulatable mechanical environment with nutrient flow through the endothelial channel that can be perfused with neutrophils. This model is the base for the development of the Cystic Fibrosis chip.

1.4 Approach

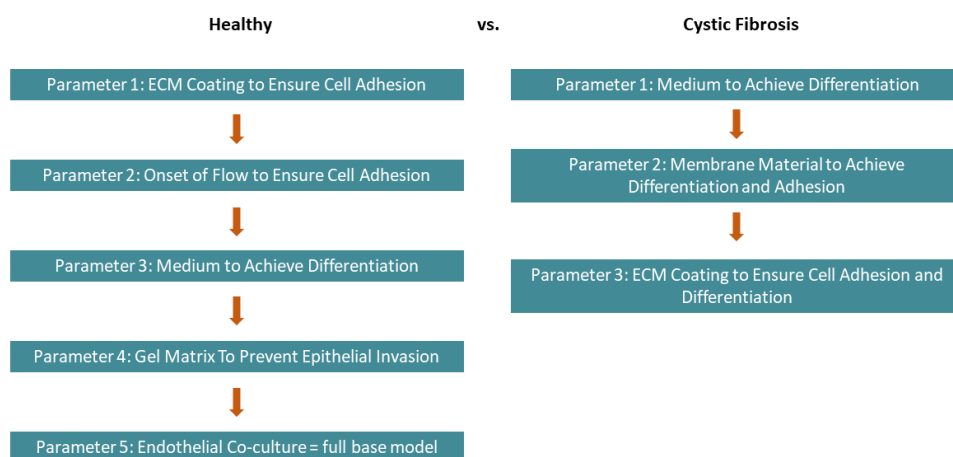


Figure 2 Steps in Model Development

The main goal of this project is to develop a differentiated Cystic Fibrosis epithelial cell culture on a chip. While the healthy airway culture on a Emulate S-1 chip undergoes optimization the

obtained knowledge of the healthy model is used to develop the diseased model (fig 2). **At the time of writing this report the research is still in progress and results are preliminary.**

2 Materials and Methods

2.1 Organ Chips

Four different *in vitro* cell culture platforms were used to differentiate airway epithelial cells (fig 3). Transwell plates (Corning, USA) were used as static 2D controls where a transwell insert with a permeable 0.4 μm pore polyester membrane is hanging into a well. The resulting two compartments can be accessed independently and allow for submerged culture conditions and air liquid interface. Organ-chips were provided by Emulate Inc. The stretchable Organ-Chip S-1™ consists of a top channel and a bottom channel that are separated by a porous membrane and dynamic laminar flow conditions can be set independently for both channels. Two different types of membranes were used. The standard S-1 design carries a 7 μm pore polydimethylsiloxane (PDMS) membrane and the alternative design⁵² makes use of a polyethylene terephthalate (PET) with pores exhibiting an average diameter of 3 μm . The PET membrane is stiffer compared to the PDMS membrane but due to its fabrication leading to random distribution of the pores and occasionally merging of pores, the pore size can vary from 3 μm to up to 10 μm . The pores in the PDMS membrane are hexagonally packed and distributed evenly. Another benefit of the PDMS membrane is its optical clarity which is limited in PET and can hinder optical readouts. The Open Top Chip (still under development) has a spiral microfluidic bottom channel and a top channel leading through a hard-plastic gasket that connects to an open chamber. The open chamber can easily be accessed by removing the gasket and sits on top of the spiral of the bottom channel. The two channels are divided by a 7 μm pore PDMS membrane.

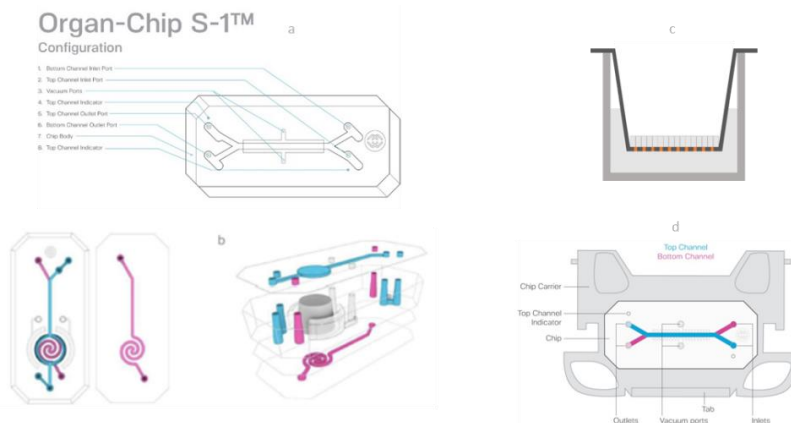


Figure 3 Cell Culture Platforms a) S1-Chip Design with PET or PDMS membrane b) Open Top Chip Design with PDMS membrane c) transwell with PET membrane d) S1-Chip in chip carrier

Top Channel	
Width x height dimensions	1000 μm x 1000 μm
Area	28.0 mm^2
Volume	28.041 μL
Imaging distance from bottom of chip to top of membrane	850 μm
Bottom Channel	
Width x height dimensions	1000 μm x 200 μm
Area	24.5 mm^2
Volume	5.6 μL
Membrane	
Pore diameter	7.0 μm
Pore spacing	40 μm (hexagonally packed)
Thickness	50 μm
Co-Culture Region	
Area	17.1 mm^2

Table 1 Dimensions of the S1-Chip

The base model of the airway chip (fig 4) consists of a mucociliary airway epithelium in the top

S1 Base Model

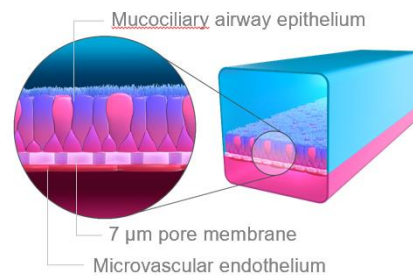


Figure 4 Emulate S1-Chip with Airway Culture: The top channel and bottom channel are separated by a 7 μm pore PDMS membrane. The top channel houses the mucociliary airway epithelium and microvascular endothelium is seeded to the bottom channel. Both channels can be perfused with different fluids/air and at different flowrates.

channel or chamber for OT-Chip and a microvascular endothelium in the bottom channel. The top channel is submerged or kept at air under static conditions for differentiation and the bottom channel is constantly perfused with fresh medium mimicking human vessels.

2.2 Instrumental Setup

The Human Emulation System of Emulate Inc. was used to perform the on-chip experiments. The components of the Human Emulation System consist of a Pod™ that houses the organ-chip, the Zoë-CM1™ module that provides pressure driven laminar flow as well as stretch and the Orb-

HM1™ that delivers a mix of 5% CO₂ with air, vacuum and power (fig 5). The top and bottom channel reservoirs of the Pod hold up to 4 ml of medium that reaches the chip trough an embedded microfluidic resistor. The Pod is equipped with a window above the chip that allows for imaging. Apart from its function as media reservoir it also serves as the interface between chip and Zoë. Zoë holds up to 12 chips, provides independent laminar medium flow for top and bottom channel and supplies vacuum for mechanical stretch at selectable frequencies and amplitudes. Zoë also features a prime cycle, that primes the microfluidic channels of the Pod and creates liquid droplets on the ports for chip connection, and a regulate cycle, that applies pressure to chips and Pods to eliminate any air bubbles in the system that could interfere with medium flow. The mix of 5% CO₂ and air for medium flow as well as vacuum (-70kPa) for stretch is provided through the Orb that forms a hub for up to four Zoës.

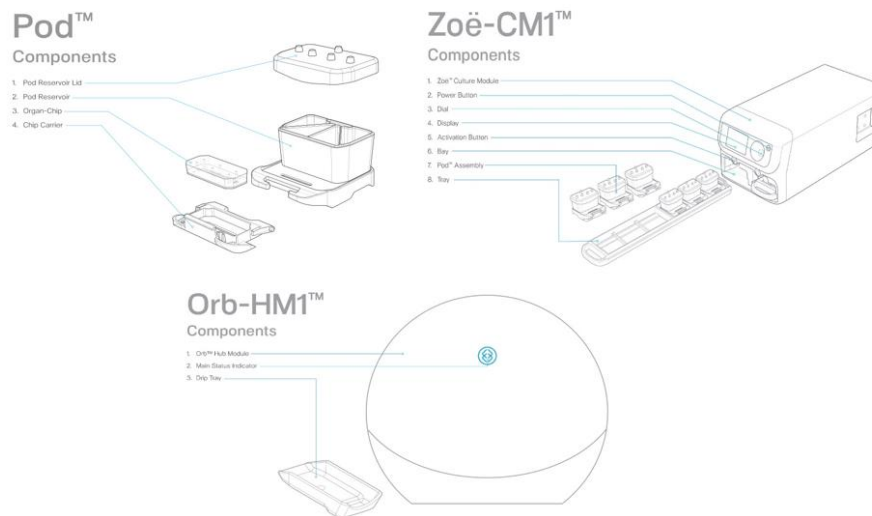


Figure 5 The Human Emulation System Components Pod, Zoë and Orb

The flowrates can be set for both channels individually (fig 6). In case of the Airway chip flowrates are set to 30 µL per hour for both channels during submerged phase and 0 µL per hour on the top channel and 30 µL per hour on the bottom channel at air liquid interface. The low flowrate of 30 µl per hour is achieved by making use of pulse width modulation (PWM) where 2.2 kPa or 0 kPa are applied to the Pods at a period of 10 seconds resulting in an average flow rate of 30 µl per hour. The peak pressure has a duty cycle of 17.4%. The applied pressure drops significantly due to the long microfluidic resistor (60 cm) before entering the chip where it is close to zero. No pressure is applied to the outlet reservoirs during regular flow. The resistance is given as PodID (PodID = 54) and equals $\frac{1}{R}$ when used in Ohm's law to calculate flowrates (Q).

$$Q = \frac{\Delta P}{R} \leftrightarrow Q = \Delta P \cdot PodID$$

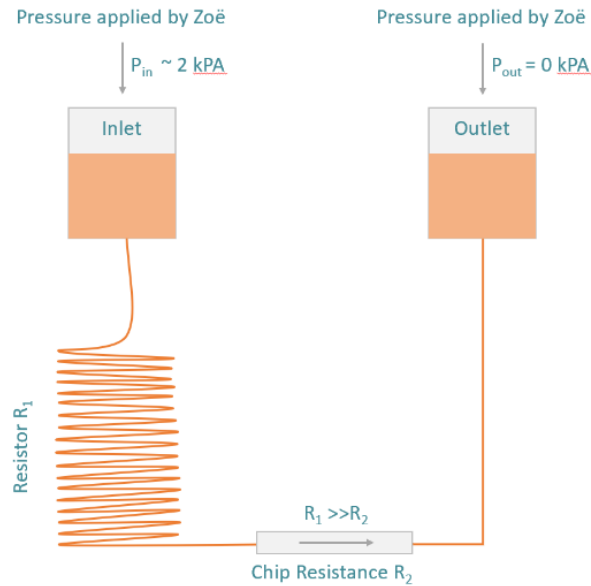


Figure 6 Schematic flow circuit for one channel

2.3 Chip Fabrication

The ready-to-use S1-Chip with 7 μ m pore PDMS membrane was provided by Emulate Inc. whereas the S1-Chip with 3 μ m pore PET membrane and the Open Top Chip with 7 μ m pore PDMS were fabricated by hand. The parts of the chip consist of a PDMS component containing the top channel, a PDMS component containing the bottom channel and the respective membrane. The PDMS parts were replica molded as described previously^{38,53}, by pouring PDMS (Sylgard, base:curing agent ratio is 10:1) into 3D printed molds (Fineline, USA) and over-night curing at 60°C. The 3 μ m pore PET sheets (AR Brown, USA) were laser cut into rectangles with 2 mm diameter holes for the ports and the resulting membrane cleaned from debris and plasma treated. After plasma oxidation the membrane was functionalized with bis[3-(trimethoxysilyl)propyl]amine), washed in IPA and rendered hydrophilic in 70% ethanol as previously described⁵⁴. The functionalized membrane was bonded onto the plasma-treated PDMS chip parts aligning ports and channels under the microscope. The resulting dimensions are described in table 1. The PDMS components of the Open Top Chip were replica molded and the 7 μ m pore PDMS membrane was obtained using soft lithography. The parts were bonded using plasma treatment.

After alignment under the microscope the channel ports were cleared of the membrane using tweezers. The gasket was 3D-printed in raisin.

2.4 Healthy primary airway epithelial cell culture

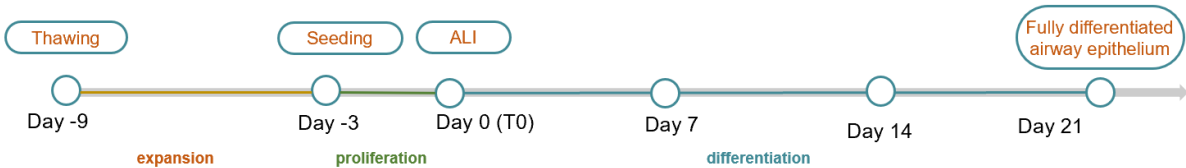


Figure 7 Basic Primary Airway Epithelial Culture. Primary cells are expanded in T75 flasks and harvested after 5 days. The cells are seeded onto the culture platforms and kept submerged for 3 days. Afterwards air liquid interface is introduced to start the differentiation process that lasts for 21 days.

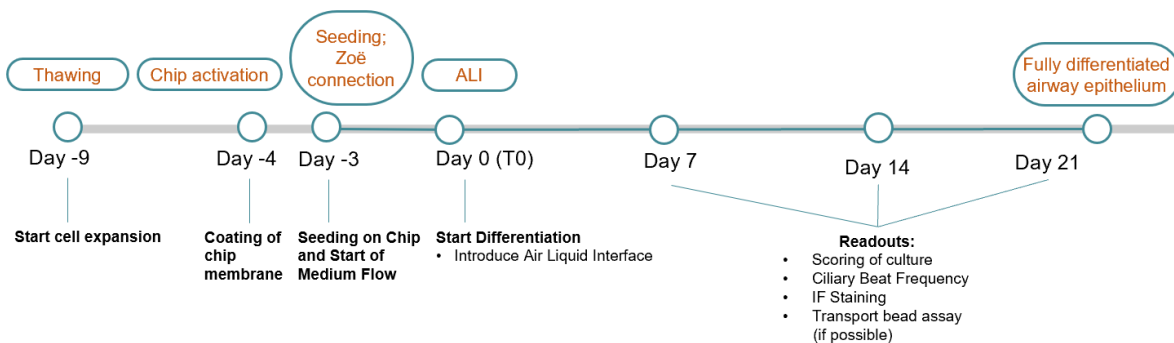


Figure 8 Timeline of Airway Chip culture. Before seeding cells onto the chip, the chip is activated by rendering membrane hydrophilic during the last day of expansion and coated with ECM. Cells are seeded onto the chip and the chips are connected to Zoë. After 3 days of medium perfusion in both channels air liquid interface is established by introducing air to the top channel.

2.4.1. Cell Expansion

Primary normal human bronchial airway epithelial cells (PBECS) and primary normal human small airway epithelial cells (SAECs) were purchased from Lifeline[®] Cell Technology or were generously provided by the Department of Pulmonology of the Leiden University Medical Center. Cells were expanded in a tissue culture treated T75 flask in small airway epithelial cell growth medium (SAGM[™] BulletKit[™], Lonza) and Gentamycin from the SAGM SingleQuots[™] supplements was replaced with 1% Penicillin-Streptomycin (Millipore Sigma). Medium was changed the day after seeding and then every other day. After five days (90 – 95% confluency) the cells were trypsinized and resuspended in serum-containing ALI medium (table 1) to stop trypsinization. The cells were centrifuged at 200 X g for 7 minutes at 24°C.

The cell pellet was diluted to a seeding density of 3,000,000 cells/mL for chip cultures and 300,000 cells/mL for static controls on transwell® (Corning Costar) plates. To optimize the cell culture condition for full epithelial cell differentiation on the S-1™ Chip, different medium conditions (table 1) were tested and cells were diluted to desired seeding densities in respective media.

Medium	Reagent	Volume	Source	Cat. No.	
Complete PneumaCult™	PneumaCult™-ALI Basal medium	500 mL	StemCell Technologies	05001	
	PneumaCult™-ALI 10X Supplement		StemCell Technologies		
	PneumaCult™-ALI Maintenance Supplement	5 vials	StemCell Technologies		
		Heparin		StemCell Technologies	07980
		Hydrocortisone		StemCell Technologies	07925
		Penicillin-Streptomycin	5 mL	Sigma	P4333
Medium	Reagent	Volume	Source	Cat. No.	
Complete ALI Medium	Gibco DMEM/F-12	500 mL	Gibco	10565-018	
	KO serum replacement	5 mL	Lonza	10828010	
	Fetal bovine serum (FBS)	5 mL	Sigma	F4135 or F8317	
	Bulletkit supplements	Everything except Gentamycin, BSA, RA, EGF	Lonza	CC-4124	
		Penicillin-Streptomycin	5 mL	Sigma	P4333
Complete “Leiden” Medium	Gibco DMEM	500 mL	Gibco	10569-010	
	BEBM base	500 mL	Lonza	CC-3171	

	HEPES	12.5 mL of 1M solution in 500mL DMEM	Gibco	15630086
	BSA	750 µL of 0.1% BSA solution per 500 ml medium bottle	Gibco	15260037
	Bulletkit supplements	Everything except Gentamycin, BSA and RA	Lonza	CC-4124
	Penicillin-Streptomycin	5 mL per 500 mL medium bottle	Sigma	P4333
Complete “Leiden” 1/5 hEGF Medium	Gibco DMEM Glutamax	500 mL	Gibco	10569-010
	BEBM base	500 mL	Lonza	CC-3171
	HEPES	12.5 mL of 1M solution in 500mL DMEM	Gibco	15630080
	BSA	750 µL of 0.1% BSA solution per 500 ml medium bottle	Gibco	15260037
	Bulletkit supplements	Everything except Gentamycin, BSA and RA	Lonza	CC-4124
	Penicillin-Streptomycin	5 mL per 500 mL medium bottle	Sigma	P4333
	hEGF (Bulletkit supplements)	100 µL of EGF (not all 500 µL)		

		per 500 ml medium bottle		
Mix 250 mL DMEM with 250 mL BEBM				

Table 2 Differentiation Media Composition

2.4.2. Transwell Controls

Cells were seeded at a density of 2344 cells/mm². Specifically, 200 µl of a cell suspension with 300,000 cells/mL, i.e., 75,000 cells total, was seeded onto 6.5 mm diameter tissue culture-treated transwell® inserts with 0.4 µm pore PET membranes. Media in the apical and basal compartment were refreshed the next day and cells were kept submerged for 3 days to allow proliferation and the formation of a tight monolayer. Three days after seeding, air liquid interface (ALI) was introduced to start epithelial cell differentiation by aspirating the medium on the apical side and refreshing the medium in the bottom well (figure 7). Maintenance was performed every other day with an apical wash and media refreshment. Apical wash consisted of incubating the top well with warm Phosphate buffered saline (PBS) for 10 min and then aspirating it to remove accumulated mucus. Cell morphology was monitored during maintenance and on day 7, 14 and 21 of ALI.

2.4.3. S-1™ Chip cultures

The chip culture is sectioned into chip activation and coating, seeding, connection of the chips to the pod, submerged culture phase and air liquid interface (fig 8).

Chip activation

Polydimethylsiloxane (PDMS) is inherently hydrophobic but it can be rendered hydrophilic by chemically activating the surface to allow the attachment of extracellular matrix proteins that provide an anchor for the cells and hence their attachment to the microfluidic chip. This chemical activation was achieved by introducing a mixture of proprietary compounds ER-1 and ER-2 (Emulate Inc.) at a concentration of 1 mg/mL into the channels, followed by exposure to UV-light for 10 mins. After the UV treatment, the chips were washed twice with ER-2. This activation process was repeated once more. After the final washing step with ER-2, the chips were then filled with PBS (Sigma).

ECM coating

To optimize epithelial cell adherence to PDMS membrane, different extracellular matrices (ECM) were tested.

For thin ECM coatings, the PBS in top and bottom channel was removed and replaced with an ECM solution (composition dependent on condition tested (table 3)). Specifically, the ECM proteins collagen IV (Col IV; collagen from human placenta, Millipore Sigma), collagen I (Col I; FibriCOL, Advanced BioMatrix), Fibronectin (Millipore Sigma) as well as bovine serum albumin (BSA) (7.5%, Gibco) were diluted in cold PBS at desired concentrations and immediately introduced into both channels of the chips. To ensure undisturbed settling of the ECM components onto the membrane for coating, the chips were incubated overnight at 37°C in a humidified petri dish.

To prepare 20-50µm thick ECM gels (e.g. to generate a softer cell substrate, or for preventing cell migration between channels), the PBS was removed only from the top channel and Col I/IV hydrogels were introduced to the top channel. Col I/IV hydrogels were prepared using 0.5 mg/mL of collagen I and collagen IV PBS. The hydrogel and the collagen components were kept on ice until introduction into chip. PBS was retained in the bottom channel. Gels were incubated overnight at 37°C. The next day a gravity flush with PBS was performed by inserting an empty 200 µl filter tip into the top channel outlet port and a 200 µl filter tip filled with PBS kept at 37°C into the inlet port. Subsequently, the chip was flushed twice with warm PBS using an electronic pipette with 100ul at a speed level 6 and a pause interval of 5 sec.

ECM coating	Concentration
Col IV	300 µg/mL
Col I + Col IV	100 µg/mL + 300 µg/mL
	300 µg/mL + 100 µg/mL
Col I + BSA	300 µg/mL + 0.1 mg/mL
Col I + Fibronectin + BSA	100 µg/mL + 50 µg/mL + 0.1 mg/mL
	300 µg/mL + 16.66 µg/mL + 0.1 mg/mL
BSA	0.1 mg/mL
Col I + Col IV Gel	0.5 mg/mL + 200 ug/mL
Col IV Gel	1 mg/mL
Col IV + Matrigel Gel	400 ug/mL col-IV + 200 ug/mL Matrigel

Table 3 ECM conditions

Seeding

Prior to seeding, the bottom channel of the chips was filled with cell culture medium and placed into the incubator to equilibrate the medium. The cells were diluted to a suspension of 3,000,000 cells/mL resulting in a seeding density of 3000 cells/mm² and carefully seeded to the top channel via the top channel inlet port. The chips were quickly inspected under the microscope to confirm a homogeneous distribution of cells and placed into the incubator for 4 hours to allow the cells to settle and adhere. After 4 hours, the top and bottom channels were gently washed with fresh medium to remove non-adherent cells and debris and placed back into the incubator for another 2 hours before connection of the chip to the Pods and subsequently to the Zoë.

Connection to Pod

Steriflip® filters (Millipore) were used to de-gas media by attaching the filter units to 50 mL Falcon tubes containing warm medium and connecting to vacuum pumps. Vacuum was applied for 15 min to eliminate excess gas from media and prevent bubbles from being formed and trapped in the chip. After 15 min the assembly was disconnected from the vacuum pump and medium was supplemented with retinoic acid (Millipore Sigma) or EC-23 (Torcis). 3 mL of medium were transferred into the top and bottom inlet reservoir of the Pod and 300 µl of medium were placed into the top and bottom outlet reservoir. The Pods were placed into Zoë and the “prime” cycle was selected. The “prime” cycle applies pressure to both inlet and outlet reservoirs resulting in the flow of medium into the manifolds and out through the Pod ports as evidenced by the formation of medium droplets on the Pod ports. These droplets are desired to ensure a liquid bridge (and not an air bubble) is formed between the ports of the Pod and the ports of the chips upon connection. To further ensure liquid bridging, droplets were also placed on all ports of the chip before connection. Chips were then connected to the Pods using the plastic clamp built into the Pod. After connection, a “via wash” was performed by pipetting the medium just above the ports referred to as vias (for distinction from chip ports) of the reservoirs and releasing it on the wall of the Pod. This removes any potential air bubbles blocking the via and preventing medium flow into and out of the chips.

Connection to Zoë

After the via wash, the chip containing Pods were placed into the Zoë using the two Zoë trays. Each Zoë can maintain a total of 12 chips, with 6 chips per tray. The volumetric flow rates of top and bottom channel were set to 30 µL/h and the “regulate cycle” was selected. The regulate cycle takes two hours and pressurizes the inlet and outlet reservoirs to increase the concentration of gas that the liquid can dissolve, leading to the reduction and dissolution of air bubbles that may

be present and could not be dislodged manually or are not visible by eye. After the regulate cycle, which takes two hours, Zoë automatically switches to regular perfusion of the chips with medium using the indicated volumetric flow rates.

Submerged Phase

One day after connection another via wash was performed and the regulate cycle was selected again. Medium was changed the day after and the waste medium collected in the outlet reservoirs was aspirated.

Air Liquid Interface

Air liquid interface was introduced 3 days after seeding. For this purpose, medium was completely removed from the top channel reservoirs and also from the bottom outlet reservoir. The chips were placed back to Zoë and the top and bottom channel volumetric flow rates were set to 1000 $\mu\text{L/h}$ and connected for roughly 1 minute, thereby introducing air into the top channel. The medium removed from the top channel was aspirated and a medium plug of 1 mL was added to the top in- and outlet reservoirs. The medium plug is used to counteract the hydrostatic pressure increase over time resulting from the collection of waste medium in the bottom channel outlet reservoir. Unless counterbalanced, the waste-mediated pressure acts on the bottom channel and filtrates fluid into the top channel, which can be harmful to the cells and submerge the air liquid interface, creating edema-like conditions. In addition, the medium plug prevents continuous evaporation from the top channel and hence ensures a humidified environment for the airway cells.

Maintenance

Medium was changed every other day in the bottom inlet reservoir as well as in the top inlet and outlet reservoir that form the plugs. After each medium exchange, a via wash was performed. An apical wash for removing accumulating mucus was performed twice a week. First, the medium plugs and the waste built up in the bottom outlet reservoir were aspirated and 300 μL of warm PBS were added into the top inlet reservoir above the via. Next, the flow rates of the Zoë were set to 1000 $\mu\text{L/h}$ for both channels and flow was introduced for an average of 2 mins until the top channel submerged in PBS. Then, the cells were incubated for 10 to 30 minutes in the submerged state to dissolve the mucus. During this incubation time the morphology of the cells were monitored and assessed using phase contrast microscopy, as the cells are best visible when submerged. ALI was reintroduced by aspirating the PBS from the top inlet reservoir and flowing at 1000 $\mu\text{L/h}$ (both channels) for roughly 1 minute. The PBS in the outlet reservoirs was removed and the top channel reservoirs were sealed with 1 mL medium. Cell morphology was monitored on 7, 14 and 21 days of ALI to check for viability and function (ciliary beat).

2.5 Cystic Fibrosis airway epithelial cell culture

2.5.1. Cell Expansion

Diseased primary human bronchial tracheal airway epithelial cells (BTECs) from donors carrying mutations in the CFTR protein that cause cystic fibrosis were purchased from different vendors and tested for cell culture. A detailed list of the vendors, genetic background of donors and donor information can be found in table 4. Cells were expanded as described above for healthy cultures, the only difference being that the duration of expansion to reach ~90% confluency ranged from 4 to 16 days depending on the cell source.

Donor	Mutation	Vendor	Age	Gender	Race	Alcohol	Smoking	Medication	Additional Comments
222158	p.V470M heterozygous variant in Exon 11, p.508del heterozygous in exon11, p.L558S heterozygous variant in exon12	Lonza	28	F	C	N	N	Zyvox	Diagnosed through a sweat test, Patient admitted with shortness of breath
450918	homozygous deletion c.1521_1523 delCTT del508 in exon 11, homozygous missense mutation c.1408G>A (p.V470M) in exon 11	Lonza	25	M		Y	N	O2, Azithromycin, Sulfamethoxazole, vanomycin, flonase, cyproheptadine, pulmozyme, symbicort, ventolin, ergocalciferol, ferrous sulfate, hyper-sal 7%, pantoprazole, viokace, zenpap	n/a
16756	Cystic Fibrosis homozygous F508del	BioIVT	25	F	C	N	N	Omeprazole, Azithromycin, Colomycin, Tiotropium, Salmeterol, Salbutamol	Cystic Fibrosis, Osteoporosis, Sinusitis
FC-0103	Cystic Fibrosis homozygous F508del	Lifeline	20	F	C			n/a	Cause of Death: Anoxia

Table 4 Donor List Cystic Fibrosis

2.5.2. ECM coating

To optimize cell culture conditions different ECMs were tested. Transwell inserts were coated with 300 µg/mL collagen IV in PBS over night at 37°C one day prior to seeding according to the standard CF *in vitro* protocols for transwell cultures⁵⁵. The coating solution was removed right

before cell seeding. Collagen I gels were prepared at different concentrations (8 mg/ml, 5 mg/mL and 3 mg/mL) over ice by diluting collagen I in reconstitution buffer (1.2 g sodium bicarbonate and 3.06 g HEPES in 75 mL of 0.067 M NaOH) and adjusting the pH with 1N NaOH to a neutral pH where necessary. 50 μ L of collagen I gel was introduced to the transwell insert. In another approach gels were molded to a height of 50 μ m using a sterilized ring-shaped spacer and PDMS stamps cut out with a 6 mm biopsy punch (Stiefel). After placing the spacer into the transwell, the freshly prepared ECM solution was added. Then, the stamp was placed on top of the spacer, limiting ECM gel formation to the space enclosed by the bottom of the insert, the circular opening of the spacer ring, and the stamp surface, hence creating a defined gel height as well as an even surface. The gels were placed into an incubator at 37°C overnight and then coated with 300 μ g/mL collagen IV (as described above) for 4 hours. The collagen solution was removed prior to seeding. 10% gelatin gel was prepared two days prior to seeding over ice and 4% microbial transglutaminase (Modernist Pantry) was used to additionally crosslink the gelatin gel by forming isopeptide bonds between the proteins. The gels were stamped down using the same approach as described above. After overnight incubation at room temperature the gels were hydrated and functionalized with collagen IV using NHS-EDC crosslinking. Here, 0.4mg/mL EDC (Thermo Fisher Scientific) in sodium acetate buffer was mixed with 1.1 mg/mL NHS (Sigma) in sodium acetate buffer and 1 mg/mL collagen IV. The mix was diluted 20 times in PBS, placed over the gelatin gel and incubated overnight at 4°C.

2.5.3. Transwell culture

Cells were seeded at a density of 400,000 cells/mL, that is 100,000 cells per insert, onto 6.5 mm tissue culture-treated transwell® inserts with 0.4 μ m pore PET membranes or polycarbonate membranes for increased stiffness and maintained as described above (see: Transwell Controls). The CF cultures were kept submerged for 3 days to 10 days depending on the culture conditions and cell source until they formed a monolayer or almost complete monolayer.

2.5.4. Chip cultures

Three chip types were tested for the CF on chip culture. Healthy PBECs or SAECs were used as control. The three chip types that were potential platforms candidates included a 7 μ m pore PET membrane chip in S1 architecture, the Open Top Chip that has an easy-accessible chamber connected to the top channel, and the S-1™ Chip with a 4 μ m pore PDMS membrane.

2.5.5. Open Top Chip Culture

Prior to coating, the surface of the chamber and bottom channel of the were activated as described in section 2.4.3. The second treatment was performed to minimize failed surface activation. After removal of PBS from the chamber, the OT chips were coated with either 8 mg/mL or 3 mg/mL collagen I gel (gels were prepared as described above). The gels were stamped down to a height of 200 μm using a 3D printed stamp (printed through Protolabs) that is supported by a rectangular frame resting on the top surface of the chip while the body of the stamp protrudes into the chamber, leaving room for excess gel to evacuate the chamber. The chips were placed into a petri dish containing PBS reservoirs and the dishes were sealed and incubated at 37°C overnight. The next day the stamps were carefully removed, avoiding damage or removal of the gel, and coated with 300 mg/mL collagen IV for 4 hours. The coating solution was removed and cells were seeded at a density of 3000 cells/mm². The cells were kept static in submerged phase until the formation of a monolayer or the formation of an almost complete monolayer was observed (3 to 10 days).

Connection of Open Top Chips to Pump at ALI

Since the Open Top Chip is still under development and Zoë compatibility has not been determined, the OT chip was instead perfused using a multichannel peristaltic pump (IPC 16, ISMATEC) via PharMed® BPT 0.25mm tubing (ISMATEC). Therefore, the OT chip was placed into a plastic gasket containing the top channel. The medium in the chamber was aspirated manually using a pipette to introduce ALI. The bottom channel was connected via PharMed® BPT 0.89 mm Tubing (Cole-Parmer) to the medium reservoir and via PharMed® BPT 0.25mm tubing to the pump and ultimately to the medium waste reservoir. The top channel was connected to 5 cm PharMed® BPT 0.89 mm tubing and closed off for sterility. The flowrate was set to 0.01 mL/min, the tubing was primed with medium and the flow was started. Cells were monitored and maintained daily. Apical washes were not performed as cell cultures did not survive far enough into the differentiation process (see results).

2.5.6. S1-Chip culture

The cystic fibrosis cell culture on the chip followed the timeline of the healthy culture and underwent the same culturing steps. The activated chips were coated only with either 0.3 mg/mL col IV or 0.5 mg/mL col I/IV hydrogels determined optimal in healthy S1 culture and transwells. Different differentiation media previously tested in transwells were used.

Table 5 Media Conditions for CF Culture

Differentiation Media (ref. table 2)
Complete PneumaCult™
Complete ALI Medium
Complete “Leiden” Medium
Complete “Leiden” 1/5 hEGF Medium
Complete “Leiden” 1/5 hEGF Medium + 4% Serum (2% HyClone + 2% KO Serum Replacement)
Complete “Leiden” 1/5 hEGF Medium + 2% Serum (2% KO Serum Replacement)

2.6 Immunofluorescence Staining

Immunofluorescence staining was performed on chips and on transwells. For this purpose, samples were washed twice with PBS and fixed with 4% paraformaldehyde (Electron Microscopy Sciences) for 20 minutes. Subsequently, all samples were washed twice with PBS and incubated with a blocking buffer composed of 0.5% Triton x100 in 5% BSA in PBS for one hour at 4°C. After incubation, the samples were washed once in PBS (5 min). Chip samples were cut into three segments with a razor blade. The samples were then incubated with mixtures of the following primary antibodies: mouse monoclonal Muc5AC (Lab Vision™, Thermo Fisher Scientific, MS-145-P1, 1:500), directly conjugated monoclonal alpha tubulin (Abcam, Alexa Fluor® 594, ab202272, 1:100), rabbit monoclonal p63 (Abcam, ab124762, 1:100), mouse monoclonal CC16 (Hycult Biotech, HM2178, 1:50), mouse monoclonal ZO-1 (Invitrogen, 33-9100, 1:100), directly conjugated monoclonal ZO-1 (Invitrogen, Alexa Fluor® 594, 339194, 1:200) and mouse monoclonal CFTR C-Terminus (R&D Systems, MAB25031, 1:100). The primary antibodies were diluted in blocking buffer in varying combinations and samples were incubated with the antibody mixes at 4°C overnight. After incubation, samples were washed with PBS three times for 5 minutes each. The last wash was followed by incubation of the samples with mixes of the following secondary antibodies in blocking buffer: AlexaFluor® Plus 647 donkey anti-rabbit IgG (Invitrogen, 1:200) and AlexaFluor® Plus 488 goat anti-mouse IgG (Invitrogen, 1:200). Additionally, the samples were stained with DAPI (Abcam, ab228549, 1:200) and phalloidin 647 (Invitrogen, A22287, 1:200). The samples were incubated with secondary antibodies, DAPI and phalloidin for one hour at room temperature and then washed with PBS three times for 5 minutes. Prolong Glass Antifade Mountant (Invitrogen) was used to mount cut-out transwell membranes onto glass slides in some cases or introduced into the exposed channels of the chip parts.

2.7 Lactate Dehydrogenase Cytotoxicity Assay

Lactate dehydrogenase (LDH) levels of effluent media were measured as a qualitative measure to observe the trend of LDH quantity e.g. cell death within one experiment, as the variability of results between LDH kits is high. The kit used was the CytoTox 96® NonRadioactive Cytotoxicity Assay (Promega). Medium in the outlet reservoir was removed in the morning of the day of interest and effluent medium samples were taken after 24 hours of flow from the outlet reservoir. A positive control of LDH in PBS and negative controls for the respective medium conditions were prepared. LDH levels for effluent media were measured in duplicate. In this coupled enzymatic assay, tetrazolium salt is converted into a red formazan product. The absorbance of the red formazan product was measured using the BioTek™ Synergy™ NEO HTS Multi-Mode Microplate Reader. The absorbance was plotted in histograms to indirectly compare LDH levels. In some cases absorbance was corrected for the value of the negative control and plotted as percentage of the absorbance of the positive control.

2.8 High-Speed Video Microscopy

High-speed videos of ciliary beat and fluorescent microbead transport were taken using the Zeiss Z1 AxioObserver inverted microscope equipped with a Pecon chamber for temperature control for live imaging and an ORCA-Flash4.0 V2 high-speed camera. Prior to live imaging an apical wash was performed to remove mucus as described earlier and the Pecon chamber was heated to 37°C.

2.9 Ciliary Imaging

Cell cultures on transwells and on chips were placed onto the microscope stage. The condenser diaphragm was adjusted to achieve optimal Koehler illumination of the ciliated surface at a magnification of 40x. Further, the turret rotation thumbwheel was set to a position in between condenser annulus H and the condenser annulus PH1 to achieve oblique illumination and hence increase contrast. The microscope was controlled via the Zeiss Zen Software and the following settings were selected prior to recording: 1024 x 1024 pixels ROI, 2x2 binning, 2s recording time, exposure time 1.004 ms, resulting in a final movie frame rate of approximately 200 frames per second. Three to six movies were taken per sample on different representative areas.

2.10 Bead Transport

In order to measure mucociliary clearance, 1 μm polystyrene microspheres (FluoSpheres™, Invitrogen, red fluorescent 580/605) were diluted in warm SAGM (37°C) at a ratio of 1:1000 and, following an apical wash, the solution was transferred into the chip or onto transwell inserts. The sample was placed onto the microscope stage and the condenser was adjusted at a magnification of 10x. Following settings were selected in Zeiss Zen prior to recording: 1024x1024 pixels ROI, 2x2 binning, 13s recording time, 40ms exposure time. Three movies were taken per sample.

2.11 Image Analysis

Images were analyzed using Fiji⁵⁶ and MATLAB (MathWorks). The ciliary beat frequency for the test sample was determined using the same method as previously described by Benam et al.⁵⁷. Cilia coverage was assessed using ImageJ by thresholding the standard deviation of brightness movie stack projection and measuring the fraction of area that is taken up by the cilia. The bead movies were analyzed using the TrackMate Plugin⁵⁸ in ImageJ. Computed data of tracked bead trajectories were imported to MATLAB and analyzed statistically for velocity and other parameters.

3 Results

3.1 Emulating the Healthy Human Airway

The basis for chip culture optimization was the protocol for small-airway-on-a-chip described by Benam et al.³⁸ and further developed internally at Emulate Inc for organ chips with PET membrane. We adopted these protocols for Emulate's S-1 Chip with PDMS membrane and validated whether processes can be continued on the new culture platform. Considering the complex nature of dynamic organ-on-a-chip cultures several biological and mechanical parameters had to be optimized. In order to evaluate different parameter conditions and to be able to terminate long-term culture early if a condition was not promising, we developed a standardized visual quality control under the lead of Dr. Anne van der Does. In this quality control, we quantified six differentiation and cell viability markers and scored the cultures under investigation on a scale from 0 excellent to 3 poor. The markers are cell death, ciliation, attachment of cells to the membrane, shape and movement of the cells, overgrowth and invasion of epithelial cells in the top channel towards the other side of the membrane. Color coding (green

0 to red 3) of the final score and the rendering of heatmaps for cultures (attachment 1) allowed for straightforward assessment of promising culture conditions.

The healthy airway culture was optimized for the Emulate S-1 Chip with PDMS membrane. In order to eliminate membrane functionalization from the list of parameters that have to be optimized, the activation process was to be adapted. The aim was to establish ubiquitous adherence of ER-2 and specifically the prevention of bubble formation during UV treatment. Therefore, the common activation protocol provided by Emulate Inc was altered so that UV treatment was split in two times 10 minutes instead of 20 minutes and repeated introduction of ER-2 in between UV treatment in order to saturate the Chip with linker molecules. This resulted in the absence of bubble formation and homogenous color change of ER-2 after UV treatment throughout all chips.

Next, the extracellular matrix providing spots of adhesion for the cells underwent optimization (fig 9). Different ECM compositions and concentrations were tested as described in table 3. All ECM solutions had a pH of 7. When comparing conditions with lower collagen I concentrations and collagen IV only, all conditions had stretched and stressed cells, showed holes within the cell layer and patches of enlarged cells as well as overgrowth and cases of epithelial-mesenchymal transition (EMT) were large amounts of fibroblasts appeared. The response of the cells within each condition was highly variable and therefore not comparable to each other. Most cell death was observed in collagen I/IV coating. In another round of experiments with increased collagen I concentration and BSA only, all conditions showed overgrowth and invasion but this time all chips within one condition exhibited similar characteristics (attachment 2). Although minor holes in the cell layer were observed after seeding in chips with BSA coating only, almost no holes were visible the next day and they eventually closed. After 14 days of ALI cilia were observed under a phase contrast microscope on BSA coated chips after washing.

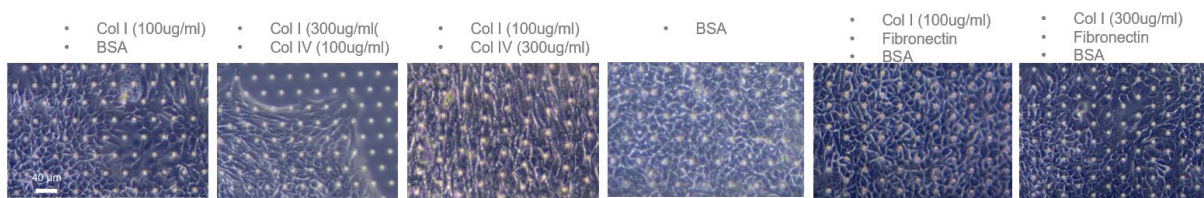


Figure 9 ECM conditions. The primary airway epithelial cells reacted drastically different to each ECM condition. Best results were observed with BSA coating and worst results were obtained using col I and col IV, as can be seen in the representative phase contrast images. Where BSA shows cobble stone morphology and col I/col IV either detaches or shows EMT.

To tackle overgrowth, invasion and movement we tested different medium conditions. The ECM conditions were tested in either complete ALI medium or complete Leiden medium. Cells grown in ALI medium detached from the membrane and displayed patches of stretched, flat and enlarged cells. Leiden medium showed good cell morphology but the chips were heavily overgrown and several cell layers formed on top of each other. To tackle this problem, we reduced human epithelial growth factor (hEGF), a supplement of Leiden medium, by 80%. There were no holes visible in the cell layer after seeding and the cell layer remained integer for 14 days after exposure to ALI. Nevertheless, these chips showed low to no ciliation and invaded cells in the bottom channel. Supplementing Leiden medium with Serum and excluding hEGF resulted in decent ciliation but detachment of cells after 10 days of ALI. To approach full differentiation, titration of retinoic acid concentration was performed with the results showing that a 100-fold increase of retinoic acid improves cell culture (fig 10). This is in compliance with the material properties of PDMS, as it has been found that PDMS has a capacity to adsorb hydrophobic and negatively charged molecules⁵⁹.



Figure 10 A 100 fold higher retinoic acid concentration than in regular transwell cultures improves cell viability and differentiation

Other media conditions tested (fig 11, 12) had D-valine DMEM/F-12 as base medium and Leiden Medium or ALI medium supplements, to prevent fibroblast proliferation that could be observed in some chips and might result from EMT⁶⁰. Cells in the medium condition D-valine DMEM/F12 plus ALI medium supplements died after 7 days, so did cells in DMEM and Leiden aliquots in the same set of experiments. D-Valine DMEM/F12 and BEBM base medium mixed at a ratio of 1:1 plus Leiden supplements showed decent ciliation and cobblestone cell shape but the chips were invaded and eventually detached in some regions. The epithelium in PneumaCult medium was heavily overgrown but after 14 days on ALI most of the cells in the top layers died and a fully ciliated monolayer appeared. At first no invasion was observed in the chip but after more than 7 days culture, cells start to appear on the other side of the membrane and throughout the bottom channel. The 50% dilution of complete PneumaCult medium with PneumaCult-ALI basal medium yielded similar results convincing with high ciliation, no movement of the epithelium, less overgrowth than 100% complete PneumaCult and almost no cell death. Both PneumaCult medium conditions enabled full differentiation at 3 weeks of ALI, however overgrowth at the start of culture and invasion was not resolved.

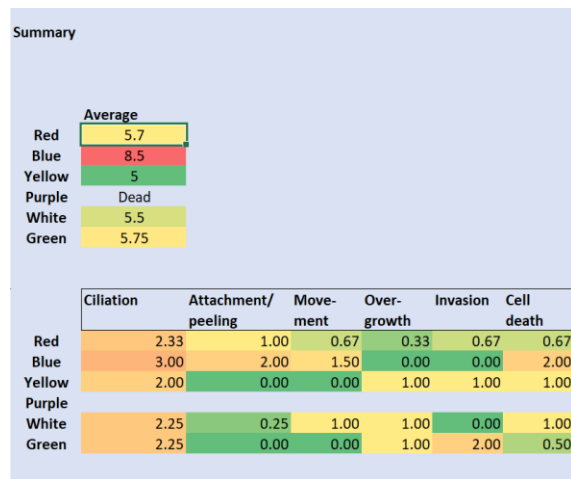


Figure 11 Scores 7 days after Introduction of ALI for several medium conditions tested in one experiment with 4 chips per condition. Conditions – red: ALI medium; blue: DMEM/HEPES + Leiden supplements; yellow: D-valine DMEM/F12/BEBM (1:1) + Leiden supplements; purple: D-valine DMEM/F12 + ALI supplements; white: PneumaCult ALI; green: Leiden 1/5 hEGF + Y-compound

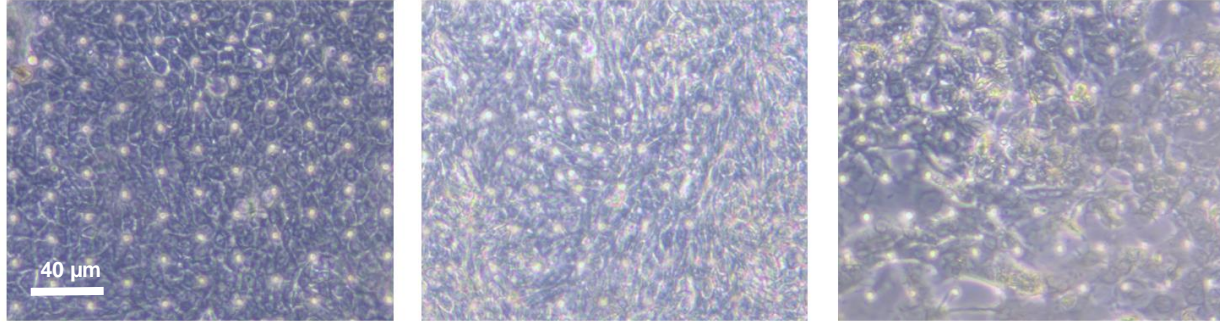


Figure 12 phase contrast images of cells grown in a) *D-valine Leiden* b) *PneumaCult* c) *ALI medium*

In order to stop cells from invading the bottom channel, introduction of gel into the top channel was tested in order to block the pores of the membrane. Thus, three different gel conditions were tested, collIV gel, coll/collIV gel and coll/Matrigel, for their effect on invasion but also on cell morphology, differentiation and viability. Collagen IV gels did not cover the entire surface of the top channel and most of the gel was removed by flushing the channel with medium (attachment 3). Nevertheless, gels do minimize migration of cells into the bottom channel (attachment 4). Out of eleven chips only one chip was fully invaded in col I plus Matrigel gels after 14 days of air liquid interface. In chips with col IV no chip was fully invaded at 14 days of ALI but sparse distribution of epithelial cells on the other side of the membrane could be observed already after 3 days on ALI. One out of four chips was fully invaded in collagen I plus collagen IV gel containing chips at 14 days of ALI and in control chips only coated with 0.1% BSA six out of eight chips displayed heavy invasion. Due to recurrent failing of the instrumentation and submersion of the cells, it is not clear whether presence of invasion and worsening of cell morphology in all conditions, observed on day 14, is due to the cells reaction to the gel substrates or rather (and more likely) wound healing processes that are triggered after repeated submersion of cells and exposure to pressure spikes and static periods of up to 10 min. Staining of the cells grown collagen I/IV gels and on collagen I/Matrigel gels revealed the presence of all major cell types of the airway epithelium (fig 13).

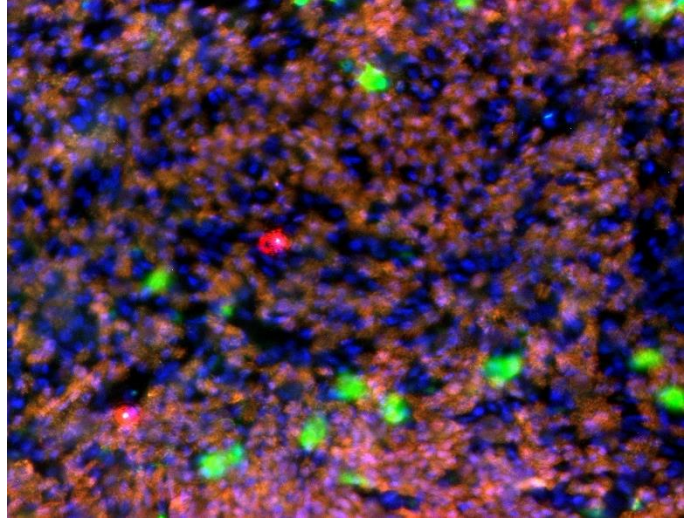
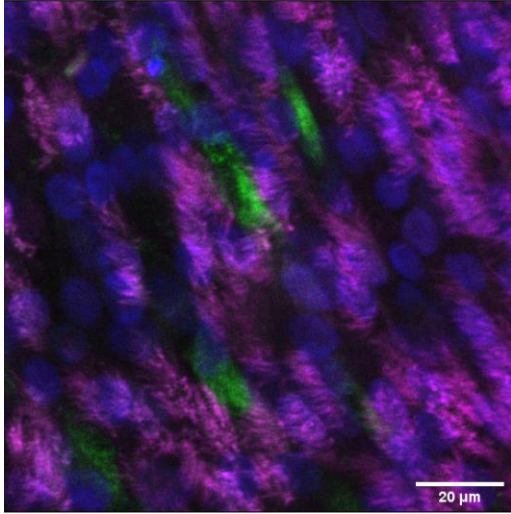


Figure 13 Staining of healthy culture growing on coll/collV gel in the S1-Chip; left: cell nuclei in blue (DAPI), goblet cells in green (Muc5AC), ciliated cells in magenta (alpha-tubulin); right: cell nuclei in blue (DAPI), goblet cells in green (Muc5AC), ciliated cells in orange (alpha-tubulin); club cells in red (CC16)

The functioning of the mucociliary escalator could be shown by bead assay and motion tracking of the beads on the airway epithelium all chips at 25 days of ALI (fig 14). Motion detection of cilia beating revealed density of cilia, which will further be used to analyze cilia coverage in all conditions and ciliary beat frequency.

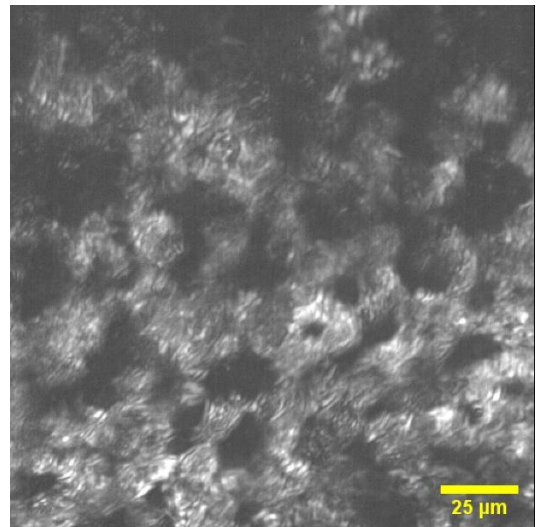
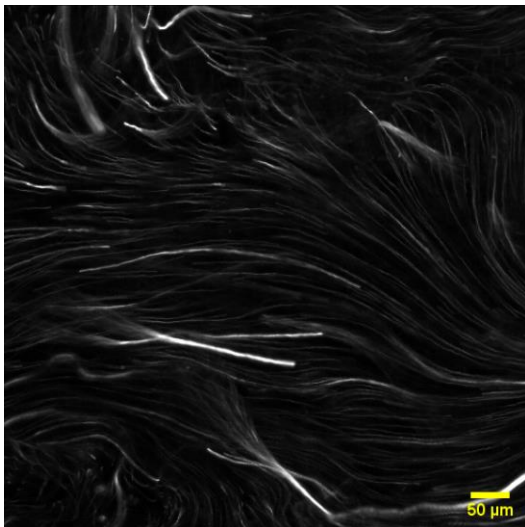


Figure 14 Motion detection revealed a) a functioning mucociliary escalator and b) cilia beating and high cilia coverage

Further, onset of flow was adapted. We tested whether a later onset of flow can improve epithelial cell viability and whether a higher flowrate can improve differentiation and viability. Therefore, we compared the PET protocol where flow is started 2 hours after seeding to 6 hours after seeding. We found that keeping the culture static for 6 hours with a refreshment of media 4 hours after seeding, improved cell viability (fig 15).

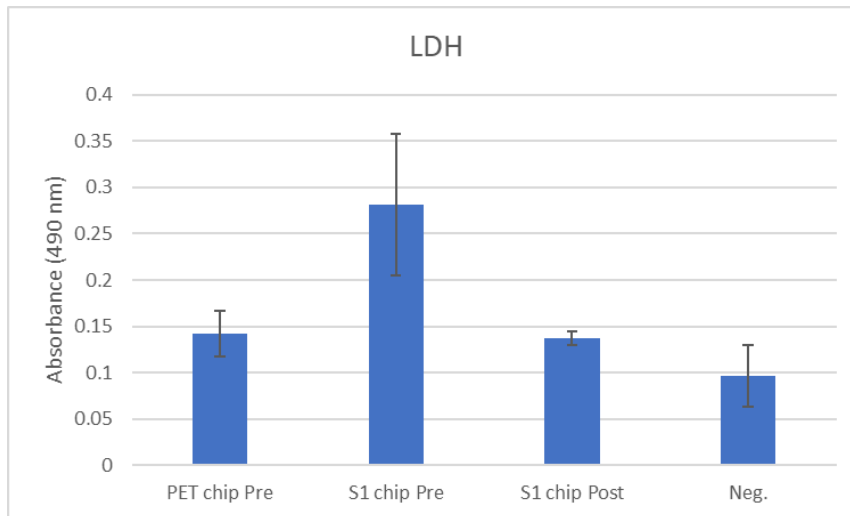


Figure 15 LDH levels of effluent - PRE = flow onset 2 hours after seeding; Post = flow onset 6 hours after seeding and refreshment of medium after 4 hours

Primary airway cultures are grown at air liquid interface which can be achieved in the chip by removing medium from the top channel and perfusing the bottom channel with media. In a closed automated system where cells are grown on porous membranes the risk of evaporation has to be eliminated and hydrostatic pressures have to be balanced. The accumulation of effluent medium in the bottom channel outlet reservoirs of the pod through perfusion leads to an increasing hydrostatic pressure that pushes against the membrane. The pressure eventually reaches a hydrostatic head that causes the flooding of the top channel and the disruption of the cell layer. To counteract the pressure, different medium plugs for the top channel in- and outlet reservoirs were tested starting with 200 μ L according to the provided protocols, 1 mL plugs modeled with the assumption of equal surface area of the inlet and outlet reservoirs (fig 16) and computed values of 1.88 mL and 1.91 mL based on the actual surface areas measured using CAD. Additionally, in one condition the top channel reservoirs were plugged with 1 mL of medium and the outlet reservoir of the bottom channel was emptied every day to create a higher hydrostatic pressure in the top channel at all times.

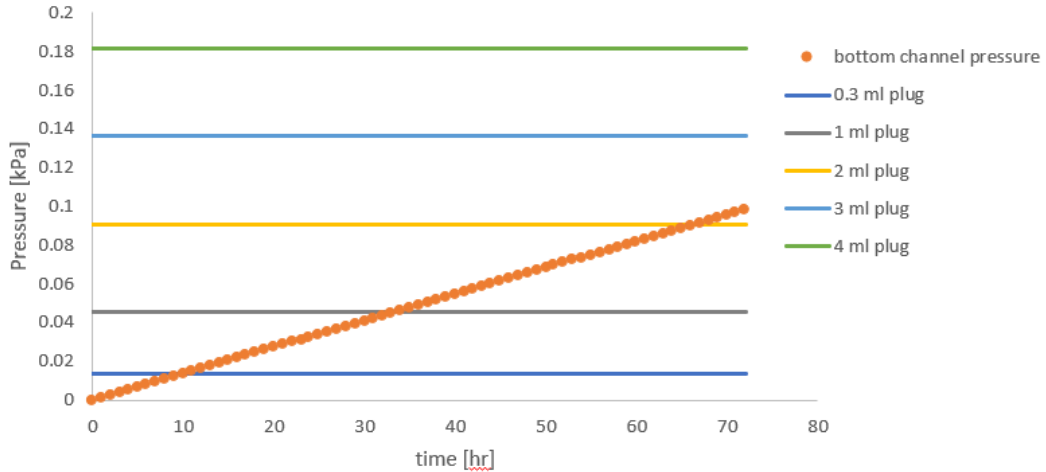


Figure 16 Comparison of pressures in top and bottom channel. The use of a 1 mL medium plug in the top channel reservoirs balances the pressure due to the waste building up in the reservoirs for up to 32h. Empirically, we found that up to 72h of continuous perfusion (and waste build-up) was supported with this protocol, likely because the cellular barrier function adds sufficient resistance to withstand the pressure differential up to this point.

Air liquid interface could not be maintained throughout a culture period of 14 days with 200 μ l plugs. The condition with the lowest (and therefore best) average score at 7 and 14 days of ALI was the condition using the exact surface areas. Yet, the condition using 1 mL medium plugs without daily removal of effluent medium convinced because of more favorable culturing processes. The scores of the individual cell differentiation and viability markers were only slightly elevated apart from one outlier, where cells detached from the membrane, raising the average score (fig 17).

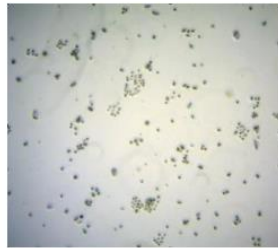


Figure 17 Average score for each pressure condition on 14 days of ALI (N=4 chips). Pressure experiments were performed in Leiden 1/5 hEGF. Conditions, A: 1.88 mL (inlet plug) and 1.91 mL (outlet reservoir) plug; B: 1 mL plug and daily waste removal; C: 1 mL plug; D: 200 μ L plug; E: 1 mL plug in 1:1 Leiden 1/5 hEGF medium and Leiden 1/5 hEGF conditioned in transwell culture of same the same donor. See attachment 5

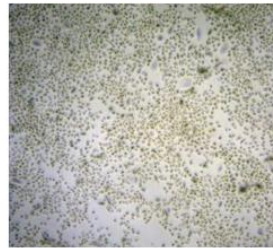
3.2 Emulating the Cystic Fibrosis Airway

Prior to chip culture, successful cell sources and culture conditions had to be determined. Therefore, all optimization processes were performed in transwells. The basis for cell culture optimization was the protocol described by Randell et al.⁵⁵, the protocol for healthy airway cultures provided by Emulate Inc. and the acquired knowledge from the optimization studies of the healthy airway. Several sources of primary human cystic fibrosis bronchial/tracheal epithelial cells had to be tested for model development. Differences in cell sources included detachment of cells from the membrane and extended cell expansion periods until ~90% confluency of 12 days in comparison to 5 days expansion for other CF cell supplies and healthy controls (fig 18). All donors were tested on collagen IV coated transwells and cultured in both Leiden and ALI medium. Successful cell sources were donor 450918 from Lonza and FC-0103 from lifeline (see table 4). Cells of these donors remained attached to the membrane of transwell inserts and differentiated showing ciliary beating and mucus secretion.

Example of confluency of plated cells after 5 days

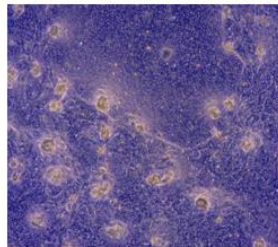


CF Cells – Supplier: BioIVT

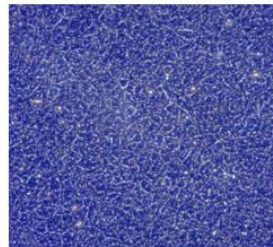


Healthy cells

Attachment of cells on transwells after 7 days on ALI



CF Cells – Supplier: Lonza



CF Cells – Supplier: Lifeline

Figure 18 Differences in cell supply – ~90% Confluency was achieved in almost all tested cell vials after 5 days but cells provided by BioIVT needed an extended expansion period of 12 days. Different cell sources were more or less likely to attach to the membrane and remain attached.

When donor 450918 was grown in ALI medium, the cell layer was very stretched and stressed. A lot of dead cells were present on top of the cell monolayer and the culture appeared “cloudy”. Cells of this donor grown in Leiden medium showed cobblestone cell morphology but were completely overgrown. Despite all that, sparse ciliation and mucus production was present in both conditions (fig 19,20).

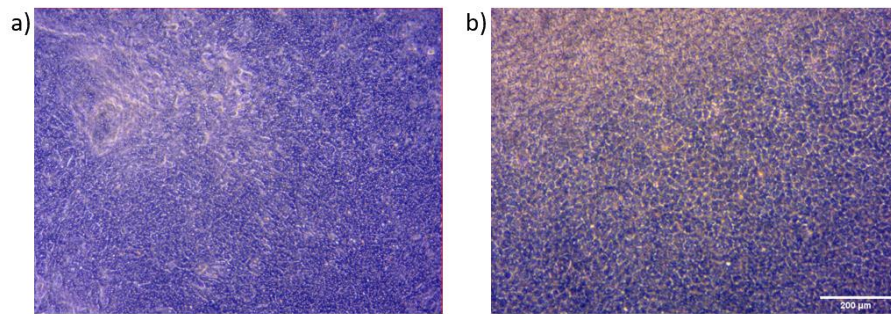


Figure 19 phase contrast image of donor 450918 a) in Emulate medium, revealing "cloudy spots" and stretched cells b) in Leiden medium, showing overgrowth but beautiful cobblestone morphology

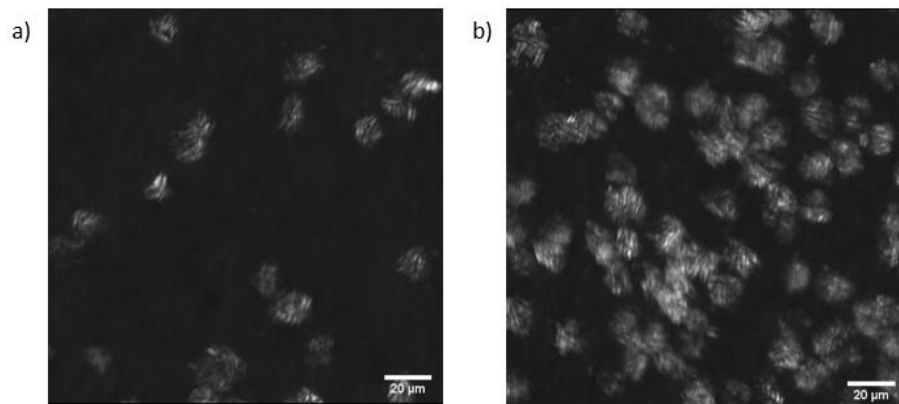


Figure 20 motion detection images of cilia a) at 15 days of ALI in ALI medium b) at 15 days on ALI in Leiden medium

Primary cells of donor 450918 were then seeded on collagen IV coated organ chips with PET membrane and 3 µm pore PDMS membrane in both medium conditions. The cells growing on PDMS retracted immediately after introduction of ALI, whereas chips growing on PET could be maintained on the chip for up to 15 days (fig 21,22).

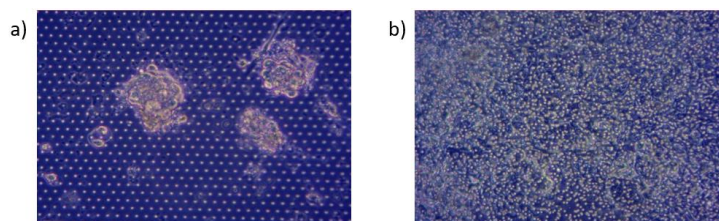


Figure 21 a) cells retracting from PDMS membrane b) cells attached to PET membrane – fibrotic, flat, cell death

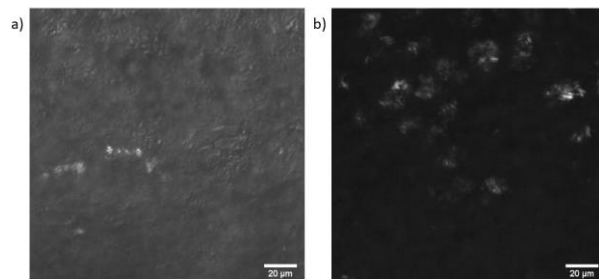


Figure 22 motion detection images on day 15 of ALI on PET Chip a) Leiden medium b) ALI medium

Due to shortage in cell supply the screening process was reinitiated and culturing of donor FC-0103 underwent optimization. Therefore FC-0103 was seeded on Col IV coated transwells and different media conditions were tested. Leiden medium and Emulate medium served as control and Leiden medium with only 20% of supplement hEGF was tested to tackle overgrowth. In addition, two other media conditions were designed to find the golden mean between Leiden medium that shows cobblestone cell morphology but heavy overgrowth and ALI medium lead to stretched, flat and squamous cells but higher cilia density. Therefore, hEGF was left out and replaced with 2% KnockOut serum in one condition and 4% Serum (2% KnockOut Serum replacement and 2% HyClone fetal bovine serum) in the other. There were no major differences observed between all adjusted conditions (fig 23). Low ciliation, cell death, patches of cobblestone cell morphology but also flat, squamous and stretched cells, reduction of overgrowth were found in all of these conditions. Cell death also appeared in healthy controls in these media.

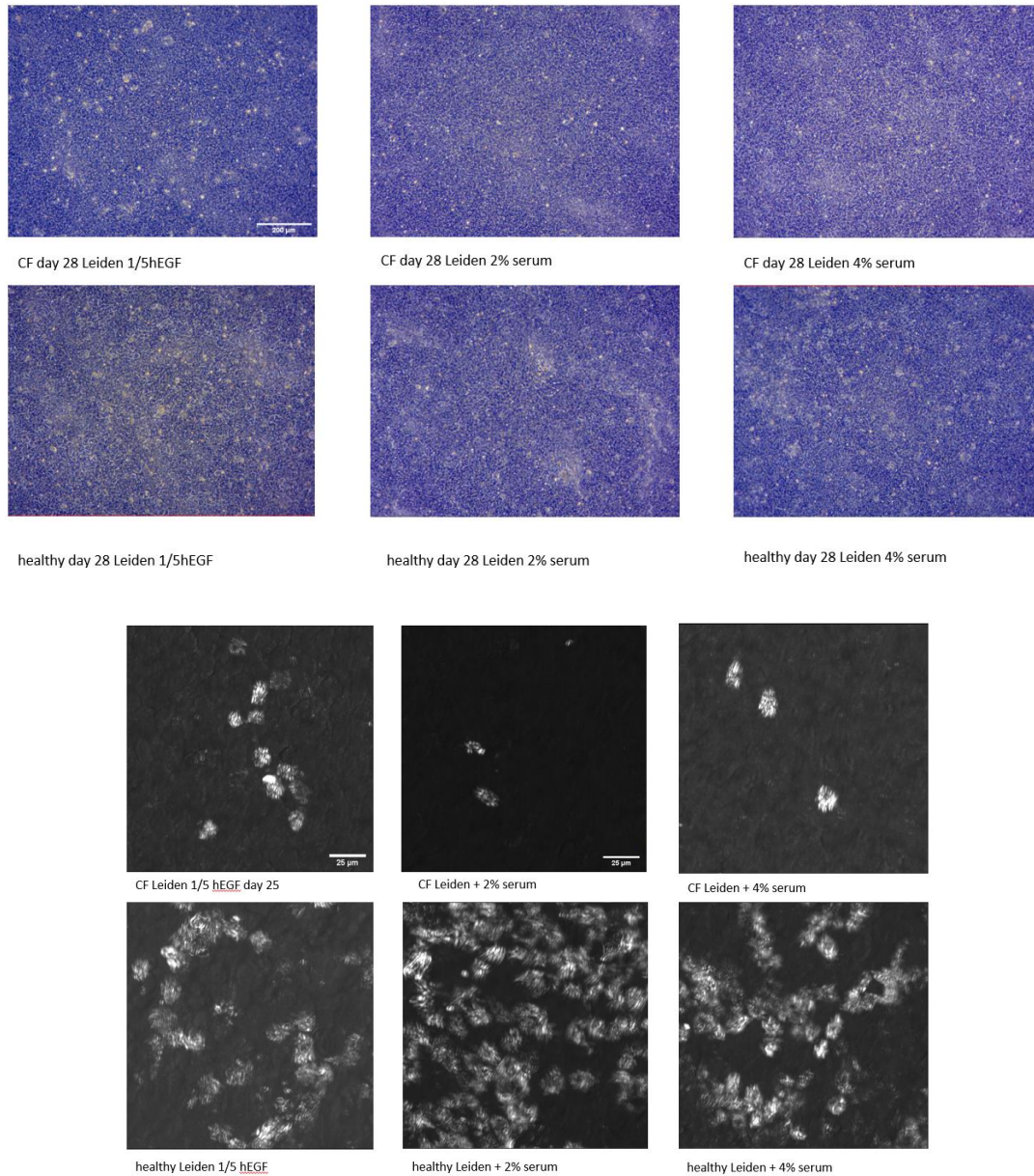


Figure 23 phase contrast images of transwell cultures in different media conditions reveal influences on cell morphology; Motion detection images reveal differences in cilia density

To further improve cell culture conditions, the use of collagen I gel coated with collagen IV instead of collagen IV coating only was assessed for its ability to positively influence cell differentiation and viability. Therefore, 8 mg/mL collagen gels were prepared for transwells, tested for their pH and stamped down to a height of 200 μm . All previously tested media conditions were investigated on these gels. In all these conditions, but Leiden 1/5 hEGF, cilia already appeared after 5 days of air liquid interface and the cultures were as densely ciliated as the healthy control by day 25 of ALI. Cells in Leiden 1/5 medium died after introduction of ALI. Although ciliation improved

drastically in all other conditions, patches of stretched cells remained and holes formed within the cell monolayer. Therefore, collagen I gel concentration was decreased to test whether a decrease in gel stiffness would influence the formation of holes and the morphology of cells. The concentrations of 8 mg/mL, 5 mg/mL and 3 mg/mL were tested in ALI medium and PneumaCult medium (during this experiment, parallel experiments in the optimization study for the healthy airway model yielded good results for the use of PneumaCult – see above). There were almost no holes visible at a col I concentration of 3 mg/mL and cilia density was similar to 8 mg/mL collagen I gel (fig 24). These two gels were tested in the Open Top Chip for CF chip model development. At a higher concentration of collagen, the gel remained attached to the chamber of the open top but holes were formed in the monolayer, the reverse is true for a low collagen I concentration (fig 25). No cultures could be kept alive for more than 7 days on the Open Top Chip.

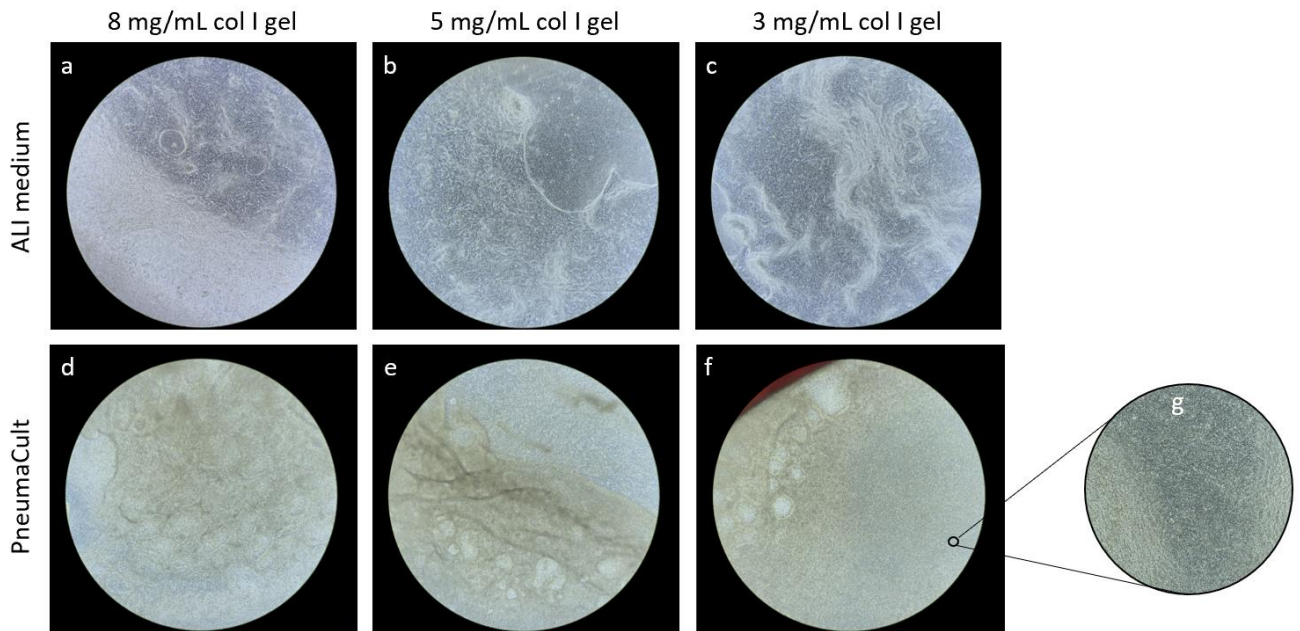


Figure 24 CF transwell cultures at 25 days of air liquid interface. Cells retract from the membrane in collagen I gels with 5 mg/mL (b,e) and 3 mg/mL (c,f). Big holes in the cell layer appear right after introduction of ALI and do not close in 8 mg/mL collagen I gels (a,d). Best morphology was observed in undetached 3 mg/mL collagen I gels in PneumaCult medium (g).

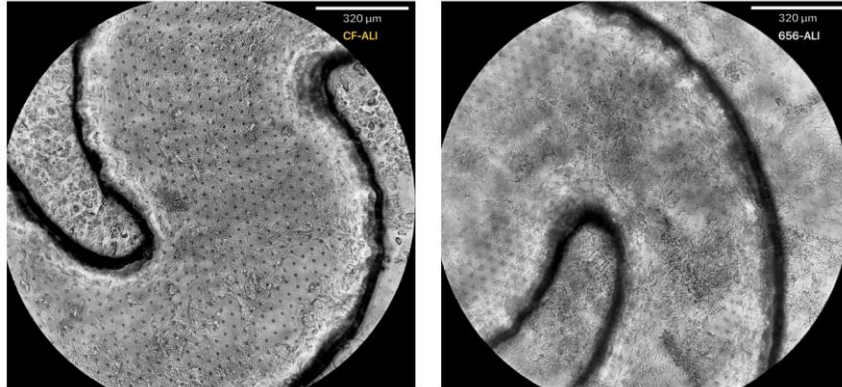


Figure 25 Open Top cell cultures grown on 8 mg/mL collagen I gels in ALI medium. Both CF and 656 show holes and patches of squamous cells and dead cells

After successful introduction of gel into the S1-Chip with 7 μ m pore membrane and differentiation of healthy cells to a mucociliary endothelium, it was assessed whether the platform switch from Open Top to S1-Chip for Cystic Fibrosis would benefit the Cystic Fibrosis culture. Based on previous findings collagen I/IV gels were introduced into the S1-Chip and CF cells were seeded in PneumaCult or ALI medium into the chip. Whereas cells growing in PneumaCult medium formed a monolayer, cells grown in ALI medium detached from the membrane and finally underwent cell death (fig 26).

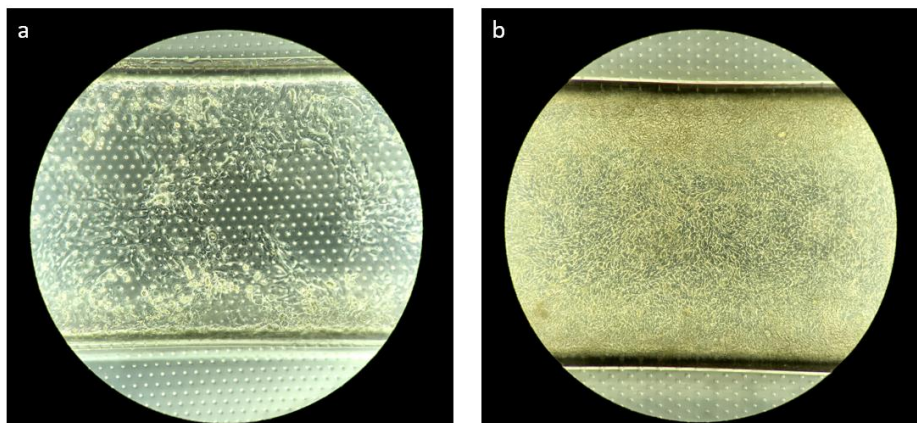


Figure 26 S1-Chip CF culture at 7 days post ALI on collagen I + collagen IV gels a) cultured in ALI medium b) cultured in PneumaCult medium

The cell cultures in PneumaCult medium differentiated showing ciliation and mucus secretion as well as all major cell types such as goblet cells, ciliated cells and basal cells of the airway epithelium already at 14 days of ALI (fig 28). Nevertheless, it should be mentioned that the gel retracted from the membrane at both inlet and outlet side but the center remained attached to the

walls. At 21 days post ALI bead assays were performed and confirmed the functioning of the mucociliary escalator as well as a high cilia density comparable to the healthy control (fig 27).

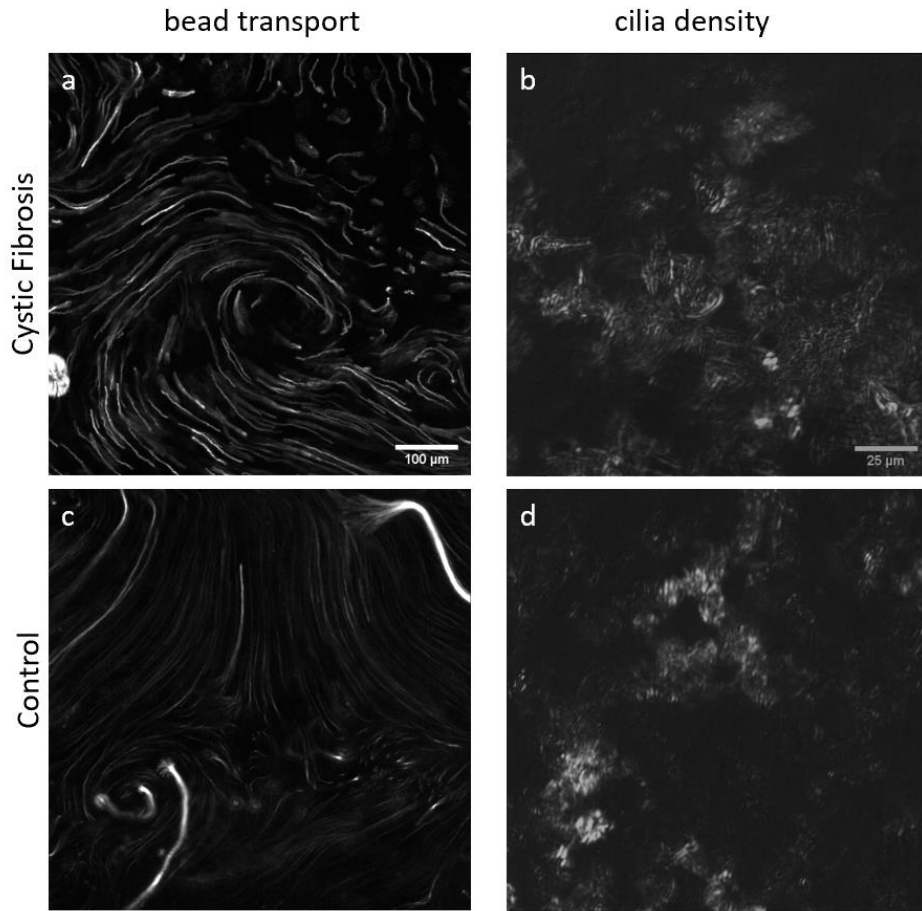


Figure 27 Visualization of the mucociliary escalator and cilia density at 21 days on ALI

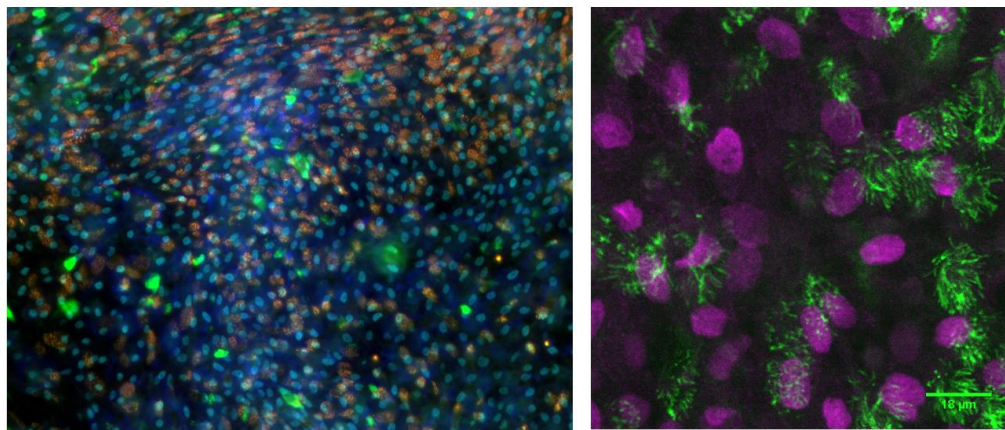


Figure 28 Validation of epithelial differentiation at 14 days post ALI; left: goblet cells in green, ciliated cells in orange, basal cells in light blue and actin in dark blue; right: basal cells in magenta and ciliated cells in green

4 Discussion

Organs-on-a-chip are complex human cell-culture platforms that aim to mimic human biology more closely than conventional cell culture models and thus add to the toolbox of translational research. A precisely defined and tunable microenvironment is crucial in model development to ensure reproducibility and relevance. This microenvironment includes the cell types involved, their hierarchy and the tissue architecture as well as mechanical forces and fluid flow that are experienced *in vivo*. Therefore, forces experienced within an automated cell culture system containing the organ chips, as used in this project, and the forces experienced in the native tissue milieu have to be determined and balanced. This is critical for tissues at air liquid interface, where the lumen experiences airflow and the endothelium experiences blood flow. Here, the top channel containing the epithelium was kept static at air and medium was perfused through the bottom channel. The build-up of effluent medium in the outlet reservoir is pushing with increasing force against the membrane that does not experience hydrostatic pressure from the top channel. These forces have to be balanced in order to prevent an environment, that can lead to inflammation, fibroblast proliferation, remodeling and ultimately result in the disruption of the epithelium. However, these manifestations of epithelia on organ chips can also appear due to improper cell isolation, ECM conditions and medium formulations. Thus, it is not straightforward to discriminate between parameters and find the root source causing these observations. Hence, two or more parameters were tested in different combinations and controls for each parameter were designed based on provided protocols. Once a parameter could be narrowed down to benefit cell viability, cell morphology, differentiation and adhesion the controls for subsequent experiments were refined. The composition and stiffness of the extracellular matrix is crucial for the success of cell cultures. Drastic differences in cell morphology and attachment were observed. Interestingly, bovine serum albumin yielded best results in ECM coating experiments prior to the use of gels. This might be attributed to its hydrophilic properties and hydrophobic pockets⁶¹ but would require to be studied in detail. Notwithstanding cell attachment to BSA coated chips, invasion occurs and patches of cell movement appear next to areas of cobblestone morphology. The introduction of gel to stop cells from invading the bottom channel by blocking the pores of the PDMS membrane has proven to be highly successful. Both gels containing collagen and gels containing Matrigel plus collagen successfully stopped epithelial cells from migrating into the vascular channel. Nonetheless, collagen gels are preferred over gels containing Matrigel because of its ill-defined composition. Continued optimization of the gels is desirable to assess which gel composition, concentration and resulting stiffnesses favor primary epithelial cell cultures both for healthy cells

as well as cells derived from Cystic Fibrosis patients. The analysis and adaptation of the mesh sizes of the different gel networks could allow neutrophil transmigration from the vascular channel through the gel to the epithelium. Moreover, the presence of gel enables mimicry of connective tissue by embedding of fibroblasts. For the establishment of the base model, that includes epithelium and endothelium, the next step would consist of the optimization of ECM coating for endothelial cells in the bottom channel, optimal shear rates for endothelial differentiation and the optimization of co-culture medium. The medium found to sustain both healthy and Cystic Fibrosis cells has to be adopted in order to additionally maintain endothelial cells. A starting point would be the use of PneumaCult medium, proven to sustain epithelium on the chips, and the supplementation of endothelial growth factors, first and foremost vascular endothelial growth factor (VEGF).

The optimized protocol for the healthy airway chip and the newly established epithelial model for Cystic Fibrosis on a chip will require to undergo further characterization to be applicable as research model. Baselines for biomarker expression, such as pro inflammatory cytokines TNF-alpha, IL- β , IL-8 and IL-6, have to be identified and confirmed to be situated within the ranges found *in vivo*, by the use of qPCR and ELISA. In order to proof robustness of the optimized protocol and exclude sensitivity based on donor-to-donor variability several donors should be tested. In the case of Cystic Fibrosis, it would be commendable to include donors with different genetic backgrounds and treatment history.

The introduction of microelectrodes to the chip or the integration of passive methods to assess CFTR function would extend the possibilities of readouts on the CF chip. Electrophysiological measurements (Ussing chamber experiments) are used to test CFTR potentiators and correctors that aim to enhance or restore CFTR function. In addition, the quantification of mucociliary clearance is an important measure to understand the cystic fibrosis lung and could be used to assess the efficacy of drugs that reduce mucus viscosity, such as Dornase alpha. The research project is at the point where mucociliary clearance is currently under investigation and quantified for the CF and the healthy airway chip.

5 References

1. Ratjen F, Bell SC, Rowe SM, Goss CH, Quittner AL, Bush A. Cystic fibrosis. *Nature Reviews Disease Primers*. 2015;1:15010 EP-. doi:10.1038/nrdp.2015.10
2. Esther CR, Muhlebach MS, Ehre C, et al. Mucus accumulation in the lungs precedes structural changes and infection in children with cystic fibrosis. *Science translational medicine*. 2019;11(486). doi:10.1126/scitranslmed.aav3488

3. Birket SE, Chu KK, Liu L, et al. A functional anatomic defect of the cystic fibrosis airway. *American journal of respiratory and critical care medicine*. 2014;190(4):421-432. doi:10.1164/rccm.201404-0670OC
4. Gustafsson JK, Ermund A, Ambort D, et al. Bicarbonate and functional CFTR channel are required for proper mucin secretion and link cystic fibrosis with its mucus phenotype. *J Exp Med*. 2012;209(7):1263-1272. doi:10.1084/jem.20120562
5. Fahy JV, Dickey BF. Airway mucus function and dysfunction. *The New England journal of medicine*. 2010;363(23):2233-2247. doi:10.1056/NEJMra0910061
6. Puchelle E, Bajolet O, Abély M. Airway mucus in cystic fibrosis. *Paediatric respiratory reviews*. 2002;3(2):115-119. doi:10.1016/S1526-0550(02)00005-7
7. Oliver A, Cantón R, Campo P, Baquero F, Blázquez J. High Frequency of Hypermutable *Pseudomonas aeruginosa* in Cystic Fibrosis Lung Infection. *Science (New York, NY)*. 2000;288(5469):1251-1253. doi:10.1126/science.288.5469.1251
8. Shei R-J, Peabody JE, Kaza N, Rowe SM. The epithelial sodium channel (ENaC) as a therapeutic target for cystic fibrosis. *Current opinion in pharmacology*. 2018;43:152-165. doi:10.1016/j.coph.2018.09.007
9. Button B, Cai L-H, Ehre C, et al. A periciliary brush promotes the lung health by separating the mucus layer from airway epithelia. *Science (New York, NY)*. 2012;337(6097):937-941. doi:10.1126/science.1223012
10. Hassett DJ, Korfhagen TR, Irvin RT, et al. *Pseudomonas aeruginosa* biofilm infections in cystic fibrosis: Insights into pathogenic processes and treatment strategies. *Expert opinion on therapeutic targets*. 2010;14(2):117-130. doi:10.1517/14728220903454988
11. Tang XX, S. Ostedgaard L, J. Hoegger M, et al. Acidic pH increases airway surface liquid viscosity in cystic fibrosis. *Journal of Clinical Investigation*. 2016;126. doi:10.1172/JCI83922
12. Berkebile AR, McCray PB. Effects of airway surface liquid pH on host defense in cystic fibrosis. *The international journal of biochemistry & cell biology*. 2014;52:124-129. doi:10.1016/j.biocel.2014.02.009
13. Pezzulo AA, Tang XX, Hoegger MJ, et al. Reduced airway surface pH impairs bacterial killing in the porcine cystic fibrosis lung. *Nature*. 2012;487(7405):109-113. doi:10.1038/nature11130
14. Rao S, Grigg J. New insights into pulmonary inflammation in cystic fibrosis. *Archives of disease in childhood*. 2006;91(9):786-788. doi:10.1136/adc.2004.069419
15. Mott LS, Park J, Murray CP, et al. Progression of early structural lung disease in young children with cystic fibrosis assessed using CT. *Thorax*. 2012;67(6):509-516. doi:10.1136/thoraxjnl-2011-200912
16. Heijerman H. Infection and inflammation in cystic fibrosis: A short review. *Journal of cystic fibrosis: Official journal of the European Cystic Fibrosis Society*. 2005;4 Suppl 2:3-5. doi:10.1016/j.jcf.2005.05.005
17. Kerem B, Rommens JM, Buchanan JA, et al. Identification of the cystic fibrosis gene: Genetic analysis. *Science (New York, NY)*. 1989;245(4922):1073-1080.
18. Riordan JR, Rommens JM, Kerem B, et al. Identification of the cystic fibrosis gene: Cloning and characterization of complementary DNA. *Science (New York, NY)*. 1989;245(4922):1066-1073.
19. Rommens JM, Iannuzzi MC, Kerem B, et al. Identification of the cystic fibrosis gene: Chromosome walking and jumping. *Science (New York, NY)*. 1989;245(4922):1059-1065.
20. ACOG Committee Opinion No. 486: Update on carrier screening for cystic fibrosis. *Obstetrics and gynecology*. 2011;117(4):1028-1031. doi:10.1097/AOG.0b013e31821922c2

21. Mickle JE, Cutting GR. GENOTYPE-PHENOTYPE RELATIONSHIPS IN CYSTIC FIBROSIS. *Medical Clinics of North America*. 2000;84(3):597-607. doi:10.1016/S0025-7125(05)70243-1
22. Iwasaki A, Foxman EF, Molony RD. Early local immune defences in the respiratory tract. *Nat Rev Immunol*. 2017;17(1):7-20. doi:10.1038/nri.2016.117
23. Sly PD, Gangell CL, Chen L, et al. Risk Factors for Bronchiectasis in Children with Cystic Fibrosis. *N Engl J Med*. 2013;368(21):1963-1970. doi:10.1056/NEJMoa1301725
24. Khan MA, Ali ZS, Swezey N, Grasemann H, Palaniyar N. Progression of Cystic Fibrosis Lung Disease from Childhood to Adulthood: Neutrophils, Neutrophil Extracellular Trap (NET) Formation, and NET Degradation. *Genes (Basel)*. 2019;10(3):183. doi:10.3390/genes10030183
25. Vandivier RW, Fadok VA, Hoffmann PR, et al. Elastase-mediated phosphatidylserine receptor cleavage impairs apoptotic cell clearance in cystic fibrosis and bronchiectasis. *J Clin Invest*. 2002;109(5):661-670. doi:10.1172/JCI13572
26. de Bont CM, Koopman WJH, Boelens WC, Pruijn GJM. Stimulus-dependent chromatin dynamics, citrullination, calcium signalling and ROS production during NET formation. *Biochimica et Biophysica Acta (BBA) - Molecular Cell Research*. 2018;1865(11, Part A):1621-1629. doi:10.1016/j.bbamcr.2018.08.014
27. Bianconi I, D'Arcangelo S, Esposito A, et al. Persistence and Microevolution of *Pseudomonas aeruginosa* in the Cystic Fibrosis Lung: A Single-Patient Longitudinal Genomic Study. *Frontiers in Microbiology*. 2019;9:3242. doi:10.3389/fmicb.2018.03242
28. Alvarez-Ortega C, Harwood CS. Responses of *Pseudomonas aeruginosa* to low oxygen indicate that growth in the cystic fibrosis lung is by aerobic respiration. *Mol Microbiol*. 2007;65(1):153-165. doi:10.1111/j.1365-2958.2007.05772.x
29. Ciofu O, Tolker-Nielsen T. Tolerance and Resistance of *Pseudomonas aeruginosa* Biofilms to Antimicrobial Agents-How *P. aeruginosa* Can Escape Antibiotics. *Front Microbiol*. 2019;10:913-913. doi:10.3389/fmicb.2019.00913
30. PILEWSKI JM, FRIZZELL RA. Role of CFTR in Airway Disease. *Physiological Reviews*. 1999;79(1):S215-S255. doi:10.1152/physrev.1999.79.1.S215
31. McCarron A, Donnelley M, Parsons D. Airway disease phenotypes in animal models of cystic fibrosis. *Respir Res*. 2018;19(1):54-54. doi:10.1186/s12931-018-0750-y
32. Rosen BH, Evans TIA, Moll SR, et al. Infection Is Not Required for Mucoinflammatory Lung Disease in CFTR-Knockout Ferrets. *Am J Respir Crit Care Med*. 2018;197(10):1308-1318. doi:10.1164/rccm.201708-1616OC
33. Brodlie M, McKean MC, Johnson GE, et al. Primary bronchial epithelial cell culture from explanted cystic fibrosis lungs. *Experimental Lung Research*. 2010;36(2):101-110. doi:10.3109/01902140903165265
34. Snoeck H-W. Modeling human lung development and disease using pluripotent stem cells. *Development*. 2015;142(1):13-16. doi:10.1242/dev.115469
35. Lancaster MA, Knoblich JA. Organogenesis in a dish: Modeling development and disease using organoid technologies. *Science*. 2014;345(6194):1247125. doi:10.1126/science.1247125
36. Dekkers JF, Wiegerinck CL, Jonge HR, et al. A functional CFTR assay using primary cystic fibrosis intestinal organoids. *Nature medicine*. 2013;19(7):939-945. doi:10.1038/nm.3201
37. Sachs N, Papaspyropoulos A, Zomer-van Ommen DD, et al. Long-term expanding human airway organoids for disease modeling. *EMBO J*. 2019;38(4). doi:10.15252/embj.2018100300
38. Benam KH, Mazur M, Choe Y, Ferrante TC, Novak R, Ingber DE. Human Lung Small Airway-on-a-Chip Protocol. *Methods in molecular biology (Clifton, NJ)*. 2017;1612:345-365. doi:10.1007/978-1-4939-7021-6_25

39. Huh D, Torisawa Y, Hamilton GA, Kim HJ, Ingber DE. Microengineered physiological biomimicry: Organs-on-chips. *Lab Chip*. 2012;12(12):2156-2164. doi:10.1039/c2lc40089h
40. Nawroth JC, Barrile R, Conegliano D, van Riet S, Hiemstra PS, Villenave R. Stem cell-based Lung-on-Chips: The best of both worlds? *Advanced drug delivery reviews*. 2018. doi:10.1016/j.addr.2018.07.005
41. Ronaldson-Bouchard K, Vunjak-Novakovic G. Organs-on-a-Chip: A Fast Track for Engineered Human Tissues in Drug Development. *Cell stem cell*. 2018;22(3):310-324. doi:10.1016/j.stem.2018.02.011
42. Huh D, Matthews BD, Mammoto A, Montoya-Zavala M, Hsin HY, Ingber DE. Reconstituting organ-level lung functions on a chip. *Science*. 2010;328(5986):1662-1668. doi:10.1126/science.1188302
43. Griffith LG, Swartz MA. Capturing complex 3D tissue physiology in vitro. *Nat Rev Mol Cell Biol*. 2006;7(3):211-224. doi:10.1038/nrm1858
44. Lu D, Kassab GS. Role of shear stress and stretch in vascular mechanobiology. *J R Soc Interface*. 2011;8(63):1379-1385. doi:10.1098/rsif.2011.0177
45. Davies PF. Flow-mediated endothelial mechanotransduction. *Physiol Rev*. 1995;75(3):519-560. doi:10.1152/physrev.1995.75.3.519
46. Davies PF, Dewey CF, Bussolari SR, Gordon EJ, Gimbrone MA. Influence of hemodynamic forces on vascular endothelial function. In vitro studies of shear stress and pinocytosis in bovine aortic cells. *J Clin Invest*. 1984;73(4):1121-1129. doi:10.1172/JCI111298
47. Levesque M. Vascular endothelial cell proliferation in culture and the influence of flow. *Biomaterials*. 1990;11(9):702-707. doi:10.1016/0142-9612(90)90031-K
48. Sidhaye VK, Schweitzer KS, Caterina MJ, Shimoda L, King LS. Shear stress regulates aquaporin-5 and airway epithelial barrier function. *Proc Natl Acad Sci U S A*. 2008;105(9):3345-3350. doi:10.1073/pnas.0712287105
49. Varner VD, Gleghorn JP, Miller E, Radisky DC, Nelson CM. Mechanically patterning the embryonic airway epithelium. *Proc Natl Acad Sci USA*. 2015;112(30):9230. doi:10.1073/pnas.1504102112
50. Li J, Wang Z, Chu Q, Jiang K, Li J, Tang N. The Strength of Mechanical Forces Determines the Differentiation of Alveolar Epithelial Cells. *Dev Cell*. 2018;44(3):297-312.e5. doi:10.1016/j.devcel.2018.01.008
51. Tang Z, Hu Y, Wang Z, et al. Mechanical Forces Program the Orientation of Cell Division during Airway Tube Morphogenesis. *Dev Cell*. 2018;44(3):313-325.e5. doi:10.1016/j.devcel.2017.12.013
52. Benam KH, Villenave R, Lucchesi C, et al. Small airway-on-a-chip enables analysis of human lung inflammation and drug responses in vitro. *Nat Methods*. 2016;13(2):151-157. doi:10.1038/nmeth.3697
53. Huh D, Kim HJ, Fraser JP, et al. Microfabrication of human organs-on-chips. *Nat Protoc*. 2013;8(11):2135-2157. doi:10.1038/nprot.2013.137
54. Christopher G. Sip, A. Folch. Stable chemical bonding of porous membranes and poly(dimethylsiloxane) devices for long-term cell culture.
55. Randell SH, Fulcher ML, O'Neal W, Olsen JC. Primary epithelial cell models for cystic fibrosis research. *Methods in molecular biology (Clifton, NJ)*. 2011;742:285-310. doi:10.1007/978-1-61779-120-8_18
56. Schindelin J, Arganda-Carreras I, Frise E, et al. Fiji: An open-source platform for biological-image analysis. *Nat Methods*. 2012;9(7):676-682. doi:10.1038/nmeth.2019

57. Benam KH, Novak R, Nawroth J, et al. Matched-Comparative Modeling of Normal and Diseased Human Airway Responses Using a Microengineered Breathing Lung Chip. *Cell Syst.* 2016;3(5):456-466.e4. doi:10.1016/j.cels.2016.10.003
58. Jaqaman K, Loerke D, Mettlen M, et al. Robust single-particle tracking in live-cell time-lapse sequences. *Nat Methods.* 2008;5(8):695-702. doi:10.1038/nmeth.1237
59. Mata A, Fleischman AJ, Roy S. Characterization of polydimethylsiloxane (PDMS) properties for biomedical micro/nanosystems. *Biomed Microdevices.* 2005;7(4):281-293. doi:10.1007/s10544-005-6070-2
60. Kalluri R, Weinberg RA. The basics of epithelial-mesenchymal transition. *J Clin Invest.* 2009;119(6):1420-1428. doi:10.1172/JCI39104
61. Huang BX, Kim H-Y, Dass C. Probing three-dimensional structure of bovine serum albumin by chemical cross-linking and mass spectrometry. *Journal of the American Society for Mass Spectrometry.* 2004;15(8):1237-1247. doi:10.1016/j.jasms.2004.05.004

6 Attachments

ATTACHMENT 1

Scoring Chart

1 Cell Death

2 Ciliation

3 Attachment

4 Movement/Shape

5 Overgrowth

6 Invasion

Cell death			
No death cells are visible on top of the cell layer	Cell death is only visible on the side channels that are not on ALI	Cell death is visible on top of the epi-layer (like cells from top channel visible)	Cell death is visible as part of the epi-layer (resulting in gaps etc.)
Ciliation			
Cilia are present throughout the epithelial layer	Cilia are present throughout the epithelial layer but low amount	Few cilia are present and/or only on the sides	No cilia are present

Discontinuity/Peeling			
The epithelium forms a monolayer throughout the chip	The epithelium looks rather disorganized and forms a monolayer almost completely throughout the chip, some gaps, visible or slight spots of peeling are present, or gaps are filled with cells	The epithelium forms a monolayer completely throughout the chip although cells are struggling with attachments and may look strange because of this	The epithelial layer is clearly peeling from several sides of the chips and/or large gaps are formed that are not filled by epithelial cells
Movement			
Cells have a cobble stone morphology, monolayer looks regular	Some parts (<30%) of the epithelium show signs of movement: stretched cells that align to each other	Around 50% of the epithelial layer has stretched and/or aligned cells	>50% of the epithelial layer has stretched and/or aligned cells
Overgrowth			
Cells form a monolayer that is well visible	Presence of cells on top of epi layer		
Invasion			
No invasion	Invaded cells have an epithelial like morphology but only here and there present	Invaded cells have an epithelial like morphology that forms layers in some or whole bottom channel	Invaded cells have a 7 threshold like morphology

ATTACHMENT 2

Scoring heat map - 5 days on ALI (Donor 656) - ECM coating

Read-out date: 2018-11-09

Position	Front of Zoe		Left tray						Right tray					
	Coating A	Coating B	Ciliation	Attachm	Move-	Over-	Invasion	Cell	Ciliation	Attachm	Move-	Over-	Invasion	Cell
	Left tray	Right tray	peeling	ment	ment	growth	death	peeling	ment	ment	growth	death		
1	6	8	3	0	1	1	1	0	3	0	1	1	1	2
2	11	8	3	2	1	1	1	3	3	0	1	1	1	2
3	6	8	3	0	1	1	1	0	3	0	1	1	1	2
4	6	8	3	0	1	1	1	0	3	0	1	1	1	2
5	6	8	3	0	1	1	1	0	3	0	1	1	1	2
6	6	8	3	0	1	1	1	0	3	0	1	1	1	2

Back of Zoe

Zoe: 128

Incubator: 1

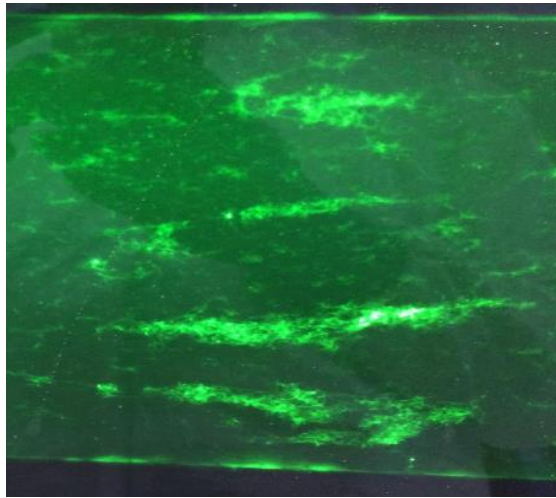
Read-out date: 2018-11-09

Position	Front of Zoe		Left tray						Right tray					
	Coating D	Coating C	Ciliation	Attachm	Move-	Over-	Invasion	Cell	Ciliation	Attachm	Move-	Over-	Invasion	Cell
	Left tray	Right tray	peeling	ment	ment	growth	death	peeling	ment	ment	growth	death		
1	14	6	3	3	3	1	1	3	3	0	0	1	0	2
2	14	6	3	3	3	1	1	3	3	0	0	1	0	2
3	14	9	3	3	3	1	1	3	3	2	0	1	0	3
4	14	6	3	3	3	1	1	3	3	0	0	1	0	2
5	14	6	3	3	3	1	1	3	3	0	0	1	0	2
6	14	6	3	3	3	1	1	3	3	0	0	1	0	2

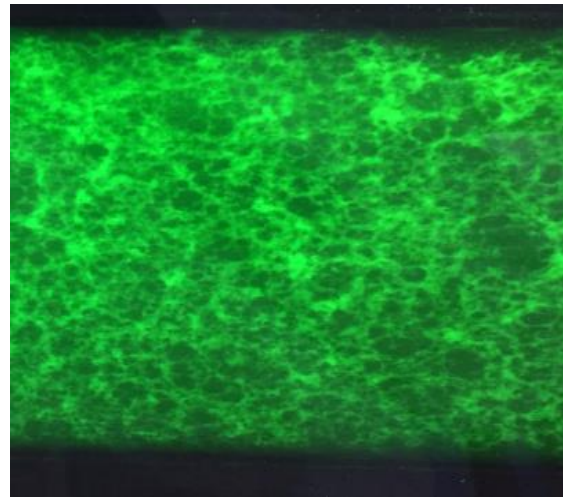
Back of Zoe

ATTACHMENT 3

Gel attachment to PDMS membrane (stained and imaged by Colleague Ibra Moulana)



Collagen IV gel (1 mg/mL)



Collagen IV (400 µg/mL) + Matrigel (200 µg/mL)

ATTACHMENT 4

Scoring heat map of healthy S1 gel conditions

Condition	Chip ID	Days Post-ALI	Peeling	Cell death	Overgrowth	Movement	Ciliation	Invasion	Score
Matrigel + Collagen IV	1.1	14	0	1	1	2.5	0	1	5.5
Matrigel + Collagen IV	1.2	14	1	1	1	2	0	0.5	5.5
Matrigel + Collagen IV	1.3	14	0	0	2	3	0	0	5
Matrigel + Collagen IV	1.4	14	2	0	2	3	0	1	8
Matrigel + Collagen IV	1.6	14	0	1	2	2.5	0	3	8.5
Matrigel + Collagen IV	1.1	14	0.5	0	1	2	0	0	3.5
Matrigel + Collagen IV	1.4	14	0	1	2	0.5	0	0	3.5
Matrigel + Collagen IV	1.6	14	2	0	0	2	0	0	4
Matrigel + Collagen IV	1.7	14	0	2	1	2	0	0	5
Matrigel + Collagen IV	1.8	14	1.5	1	1	2	1	2	8.5
Matrigel + Collagen IV	1.9	14	1	1	0	3	0	3	8
Collagen IV	2.3	14	0	1	1	2	0	1	5
Collagen IV	2.4	14	1	0	0	3	2	0	6
Collagen IV	2.5	14	0.5	0	1	1	0	0	2.5
Collagen IV	2.6	14	0	0	1	1	0	1	3
Collagen IV	2.9	14	1	0	2	2	0	0	5
Collagen I + IV	2.1	14	0	1.5	2	1	0	0.5	5
Collagen I + IV	2.4	14	0	1.5	2	2.5	0	1.5	7.5
Collagen I + IV	2.5	14	2	1	2	2.5	0	0	7.5
Collagen I + IV	2.6	14	1	1.5	1	2.5	0	1	7
Control	3.1	14	2	1	2	1	0	3	9
Control	3.2	14	0	0	3	1	0	1	5
Control	3.3	14	2	0	2	3	0	1.5	8.5
Control	3.8	14	2	0	3	2	0	3	10
Control	3.1	14	0.5	0	0.5	1	0	0	2
Control	3.2	14	0	2	1	2	0	2	7
Control	3.3	14	0	2	0	2	0	2	6
Control	3.5	14	0	0.5	0	2	0	2	4.5

ATTACHMENT 5

Scoring heat map of pressure experiments at 14 days of ALI

